



HAL
open science

Theoretical study of the coherent backscattering of light by disordered media

E. Akkermans, P.E. Wolf, R. Maynard, G. Maret

► **To cite this version:**

E. Akkermans, P.E. Wolf, R. Maynard, G. Maret. Theoretical study of the coherent backscattering of light by disordered media. *Journal de Physique*, 1988, 49 (1), pp.77-98. 10.1051/jphys:0198800490107700 . jpa-00210676

HAL Id: jpa-00210676

<https://hal.science/jpa-00210676>

Submitted on 4 Feb 2008

HAL is a multi-disciplinary open access archive for the deposit and dissemination of scientific research documents, whether they are published or not. The documents may come from teaching and research institutions in France or abroad, or from public or private research centers.

L'archive ouverte pluridisciplinaire **HAL**, est destinée au dépôt et à la diffusion de documents scientifiques de niveau recherche, publiés ou non, émanant des établissements d'enseignement et de recherche français ou étrangers, des laboratoires publics ou privés.

Classification
 Physics Abstracts
 42.20 — 71.55J

Theoretical study of the coherent backscattering of light by disordered media

E. Akkermans (*), P. E. Wolf, R. Maynard and G. Maret (¹)

Centre de Recherches sur les Très Basses Températures, C.N.R.S., 166X, 38042 Grenoble Cedex, France

(¹) Hochfeld Magnet labor, Max-Planck Institut für Festkörperforschung, 166X, 38042 Grenoble Cedex, France

(*) Also at Institut Laue-Langevin, 156X, 38042 Grenoble Cedex, France

(Reçu le 27 juillet 1987, accepté le 1^{er} octobre 1987)

Résumé. — Nous présentons une étude théorique de la rétrodiffusion cohérente de la lumière par un milieu désordonné dans diverses situations incluant les effets dépendant du temps, les milieux absorbants et les effets liés à la modulation d'amplitude de la lumière. Nous discutons tout particulièrement le cas de la diffusion anisotrope et les effets de la polarisation afin d'expliquer quantitativement les résultats expérimentaux. Nous donnons un calcul microscopique de l'albedo cohérent afin de justifier la relation heuristique précédemment établie. Nous prédisons aussi la forme de l'albedo cohérent d'un milieu fractal. Enfin, la validité des différentes approximations utilisées est discutée et quelques développements ultérieurs sont évoqués.

Abstract. — A theoretical study of the coherent backscattering effect of light from disordered semi-infinite media is presented for various situations including time-dependent effects as well as absorption and amplitude modulation. Particular attention is devoted to the case of anisotropic scattering and to polarization in order to explain quantitatively experimental results. A microscopic derivation of the coherent albedo is given which strongly supports the heuristic formula previously established. In addition the coherent albedo of a fractal system is predicted. The validity of the different approximations used are discussed and some further theoretical developments are presented.

1. Introduction.

The scattering of light by an inhomogeneous medium is an old problem which appeared at the turning of the century in the context of the study of propagation of light in the high atmosphere. This problem is very important in many fields of investigations like the scattering of electromagnetic waves from fluctuations in plasmas and more generally, turbulent media, meteorology, astrophysics and indeed condensed matter physics.

When considering the problem of propagation of waves in strongly heterogeneous media it is useful to recall briefly the different regimes for wave propagation. Three characteristic lengths are important in this problem: the wavelength λ , the scattering mean free path or extinction length ℓ and the transport mean free path ℓ^* . These mean free paths are well defined for a dilute medium of scatterers where only the single scattering is taken into account: they depend only on the cross section and the scatterers concentration. When the scattering is

isotropic ℓ is equal to ℓ^* . Otherwise, for example for scatterers of size comparable to λ , ℓ^* can be larger than ℓ . For distances less than ℓ the phase of the wave is correlated and the propagation of the light is described by a wave equation in an average medium as long as λ is shorter than ℓ . Between ℓ and ℓ^* the transport of intensity obeys an equation of the Boltzmann-type while for distances larger than ℓ^* the effective transition probability for scattering becomes isotropic and the diffusion approximation is valid. This was the basis of the radiative transfer theory initiated by Schuster [1] in 1906. In this kind of description the correlation between the phases is neglected beyond ℓ and the « random walk » of the light is described classically.

The effect of interferences over scales larger than ℓ in the multiple scattering processes was first discussed by de Wolf [2] in the context of radar scattering from ionized and neutral gases. The basic interference effect in the backscattering direction was clearly demonstrated in 1984 by Kuga and Ishimaru [3] who observed an enhancement near the

retroreflection direction of the light scattered by a suspension of latex spheres. However, possibly due to a limited experimental resolution, the enhancement was only 15 % for the largest concentration i.e. for the broadest cone, in contrast to latter experiments to be described below. In following publications Tsang and Ishimaru [4, 5] explained this observation by considering the constructive interference in the backward direction due to double [4] scattering and then multiple scattering [5]. This interference property has been called the coherent backscattering or sometimes the coherent albedo. Simultaneously solid-state physicists dealt with similar problems in the domain of electronic transport properties of impure metals. The coherent backscattering phenomenon previously evocated affects the transport cross section in the so-called «weak localization» regime. By increasing the probability of backscattering of electrons it decreases the electrical conductivity at low temperatures [6]. Modification of these interferences by applying a magnetic field provided spectacular oscillations of the magneto-resistance [7] with period of the flux quantum.

In an important paper Golubentsev [8] analysed the coherent backscattering of light within the multiple scattering situation as well as the suppression of the effect by the motion of scatterers.

A cone of coherent backscattering in two and three dimensions was predicted by Akkermans and Maynard [9] followed by a new generation of experiments by Wolf and Maret [10] and Van Albada and Lagendijk [11]. These observations of the coherent backscattering were also performed on highly concentrated suspensions of polystyrene particles in water. They revealed additional features which stimulate deepening of the theoretical analysis : the observation of peak heights close to 2, the sharp (almost triangular) lineshape of the peak, the polarization effects and the dependence on the size of the scatterers. An analysis of this lineshape has been given by Akkermans, Wolf and Maynard [12] within the diffusion approximation for the transport equation, as well as a first approach of the partial suppression of the coherent albedo for crossed orientation of incident and detected polarizations. The effects of the polarization and the transverse nature of light on coherent backscattering have been calculated in detail by Stephen and Cwillich [13] within the diffusion approximation for point-like scatterers.

An anisotropy of the cone of backscattering for small particles has been observed by van Albada, van der Mark and Lagendijk [14]. It originates from the low-order Rayleigh multiple scattering. By comparing the albedo of slabs of different thickness they were also able to determine the contributions of the different orders of scattering to the lineshape. All these features in the retroreflection of light have

been observed and analysed for ensemble averaged systems where the sampling time is larger than the characteristic correlation time of the scattered light.

On the other hand, the time autocorrelation function of the light intensity multiply scattered by the suspensions has been determined by Maret and Wolf [15] inside and outside the backscattering cone. Strong fluctuations of the intensity (speckle) were observed on solid samples. After numerical ensemble averaging of tens of scans a peak is built up in the backscattering direction as found by Etemad, Thompson and Andrejco [16]. Another, more performant way of ensemble average by rotating the samples has been reported by Kaveh, Rosenbluh, Edrei and Freund [17] with a determination of the statistical distribution of the scattered intensity. This short (and partly incomplete) review may demonstrate the rapidly growing recent interest in the field of weak localization of light.

The purpose of the present article is to give a critical discussion of theoretical foundations of the coherent backscattering and to propose new expressions of the albedo for more general situations than treated previously. The paper is organized as follows : in section 2, a heuristic expression of the averaged albedo of a disordered medium is developed for both the time dependent and the stationary regimes. Then the corrections due to modulation or absorption are established. For a comparison with the experiments it is essential to carefully discuss the effect of the anisotropy of scattering arising from large sizes of the scatterers (compared to the wavelength). In this situation, the transport mean free path ℓ^* differs significantly from ℓ : this calls for a generalization of the diffusion equation which is discussed. In section 3, we justify the heuristic expression of the albedo by a microscopic treatment of the perturbation expansion in terms of multiple scattering.

Particularly the basic interference factor $\cos [(\mathbf{k}_0 + \mathbf{k})(\mathbf{r}_1 - \mathbf{r}_N)]$ where \mathbf{k}_0 and \mathbf{k} are respectively the incident and emergent wavevectors and \mathbf{r}_1 and \mathbf{r}_N the initial and terminal points of a sequence of N scatterings, is shown to arise from the classification of the diagrams in «ladder» and «crossed» related by time reversal symmetry.

An expansion into the orders of multiple scattering is proposed in section 5. Up to this point all developments are made for scalar waves. In section 6 the vectorial nature of the electromagnetic waves is taken into account. The depolarization ratio and polarization dependence of the coherence between time reversed paths are obtained as a function of the order of multiple scattering for Rayleigh scattering. This allows us to give a physical interpretation of the recent results of Stephen and Cwillich [13] about the lineshape and to discuss them critically.

In section 7, the albedo of a fractal structure is

analysed and a simple expression involving the characteristic dimensions of the fractal structure is obtained. Finally, the main results of this paper are summarized in section 8 and some comments added.

The basic phenomenon which underlies the enhanced backscattering is the constructive interference effect in the backscattering direction. This fundamental effect can be discussed in a simple way before entering the detailed developments of the theory. For the sake of simplicity let us consider the propagation of scalar fields. In a medium of scatterers we define $A(\mathbf{R}_i, t; \mathbf{R}_j, t')$ as the complex amplitude of the field at (\mathbf{R}_j, t') from an impulse point source at (\mathbf{R}_i, t) . For the geometry of the albedo, the sources as well as the terminal points of the scattering sequences are located near the interface between the scattering medium and the non scattering medium (air, vacuum, ...). The incident and emergent wavevectors are respectively \mathbf{k}_0 and \mathbf{k} . The reflected intensity α from the medium is obtained from the product of A and A^* , weighted by the external phase factors of the incoming and outgoing waves summed over the coordinates of the initial and final points of the scattering sequences :

$$\alpha(\mathbf{k}_0, \mathbf{k}, t, t') \propto \sum_{\substack{i,j \\ t,m}} A(\mathbf{R}_i, t; \mathbf{R}_j, t') \times A^*(\mathbf{R}_\ell, t; \mathbf{R}_m, t') e^{i\mathbf{k}_0 \cdot (\mathbf{R}_i - \mathbf{R}_\ell) + i\mathbf{k} \cdot (\mathbf{R}_m - \mathbf{R}_j)} \quad (1)$$

Three contributions are included in (1). They are labelled by *i* for the incoherent multiple scattering (Fig. 1a) ; *c* for the coherent multiple scattering (Fig. 1b) and *s* for « speckle » or fluctuating contribution. These contributions can be written as :

$$\begin{aligned} \alpha_i &\propto \sum_{i,j} |A(\mathbf{R}_i, t; \mathbf{R}_j, t')|^2 \\ \alpha_c &\propto \sum_{i,j} |A(\mathbf{R}_i, t; \mathbf{R}_j, t')|^2 e^{i(\mathbf{k}_0 + \mathbf{k}) \cdot (\mathbf{R}_i - \mathbf{R}_j)} \\ \alpha_s &\propto \sum_{(i,j) \neq (\ell,m)} A(\mathbf{R}_i, t; \mathbf{R}_j, t') A^*(\mathbf{R}_\ell, t; \mathbf{R}_m, t') \times e^{i\mathbf{k}_0(\mathbf{R}_i - \mathbf{R}_\ell) + i\mathbf{k}(\mathbf{R}_m - \mathbf{R}_j)} \end{aligned} \quad (2)$$

where we have used the time reversal symmetry property :

$$A(\mathbf{R}_j, t; \mathbf{R}_i, t') = A(\mathbf{R}_i, t; \mathbf{R}_j, t') .$$

Suppose first that the scatterers are immobile. The last term provides a contribution leading to a « speckle » pattern of the intensity fluctuating over characteristic scale $\delta\theta$ of the reflection angle θ (such that $|\mathbf{k} + \mathbf{k}_0| = 2k \sin \theta / 2$), $\delta\theta \propto \lambda / D$ where D is the width of the beam of light ($D \gg \ell^*$). Suppose now that the scatterers are in a random motion and that the scattered intensity is averaged over a time large compared to the coherence time of scattered

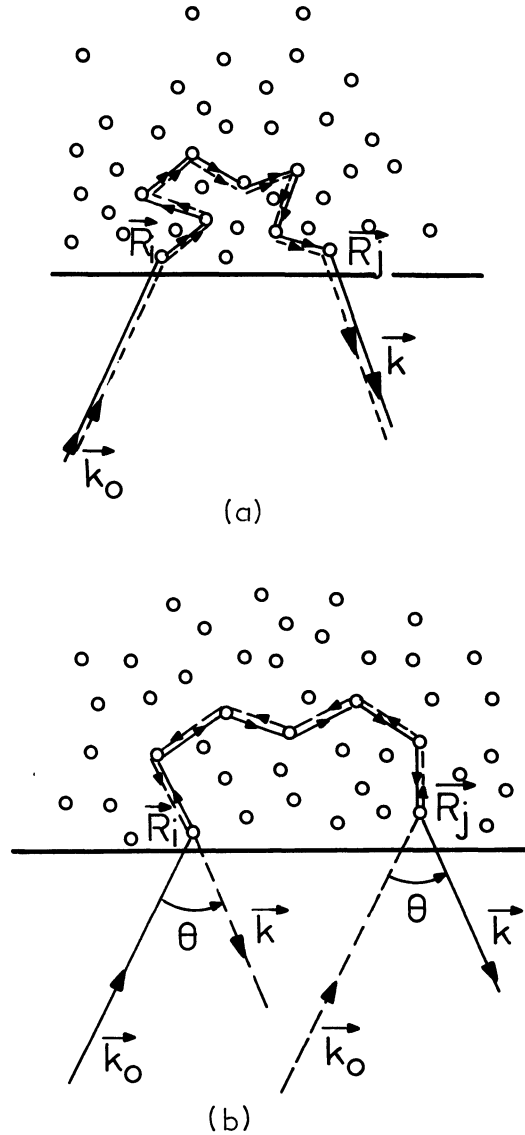


Fig. 1. — (a) Incoherent multiple scattering contribution to the total albedo; (b) Coherent multiple scattering contribution to the total albedo.

light. This condition defines an averaged medium from which the interferences of the « speckle » are washed out. Hence α_s vanishes while the two other contributions α_i and α_c subsist in average. They involve now the averaged propagator for the intensity $Q(\mathbf{R}_i, t; \mathbf{R}_j, t')$ defined by :

$$Q(\mathbf{R}_i, t; \mathbf{R}_j, t') = \overline{|A(\mathbf{R}_i, t; \mathbf{R}_j, t')|^2} \quad (3)$$

where the bar indicates that the ensemble average has been performed. The incoherent contribution α_i for the albedo is therefore obtained from this averaged propagator of the intensity Q without reference to the phases of the field amplitudes, i.e. from the radiative transfer theory describing the transport of the intensity from \mathbf{R}_i at t to \mathbf{R}_j at t' . For large number of scatterings this transport

process can be described by a diffusion process of the intensity. The coherent contribution involves a phase factor $(\mathbf{k}_0 + \mathbf{k}) \cdot (\mathbf{R}_i - \mathbf{R}_j)$ which survives the ensemble average. It originates from the particular situation described in figure 1b, i.e. from the interference between the wave travelling along any sequence and the conjugated wave travelling in reversed order along the same sequence.

Indeed time reversal symmetry relates the two paths represented in figure 1b. By gathering together both contributions, one obtains :

$$\overline{\alpha(\mathbf{k}_0, \mathbf{k}, t, t')} \propto \sum_{i,j} (1 + \cos((\mathbf{k}_0 + \mathbf{k}) \cdot (\mathbf{R}_i - \mathbf{R}_j))) \cdot Q(\mathbf{R}_i, t; \mathbf{R}_j, t') \quad (4)$$

where the interference effect is now taken into account in the term accounted for by the cosine term. The averaged albedo of disordered substances can then be calculated once the averaged propagator $Q(\mathbf{R}_i, t; \mathbf{R}_j, t')$ for the intensity transport is known. This will be carried out in the next part in different situations.

2. A heuristic expression of the albedo.

We consider in this part how the coherent backscattering effect explained in the introduction affects the angular dependence of the average reflected intensity of a scalar wave multiply-scattered by a semi-infinite disordered medium (Fig. 2). To this end, we shall first give a phenomenological derivation of the basic expression for the albedo, which will be confirmed on a microscopic basis in section 3.

Let us first study the time-dependent case in which an energy pulse is incident on the medium. The incident energy flux is $F_0 \delta(t)$ where F_0 is the pulse

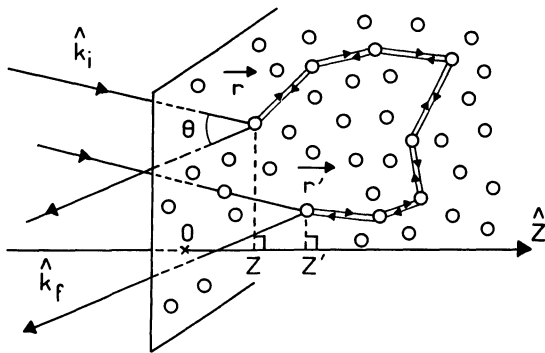


Fig. 2. — Geometry used for the calculation of the coherent albedo, showing two interfering light paths.

energy per unit surface. After the wave experiences its first collision, the total energy released per unit time in the elementary volume $d^2\rho dz$ is given by :

$$F_0 \delta(t) e^{-z/\mu_0 \ell} \frac{dz}{\ell} d^2\rho. \quad (5)$$

The transport of the light intensity in the medium is described by the Green function $P(\mathbf{r}, \mathbf{r}'; t)$ defined by the response in \mathbf{r}' at time t to a pulse in \mathbf{r} at time $t = 0$. For a large number of scatterings (or in the long time limit), this function is well approximated by the solution of a time-dependent diffusion equation. The incoherent energy emerging from the medium per unit time in the solid angle $d\Omega$ around the emergent direction \hat{s} is given by

$$\int \frac{dz}{\ell} d^2\rho e^{-z/\mu_0 \ell} F_0 c P(\mathbf{r}, \mathbf{r}'; t) \times e^{-z'/\mu \ell} \frac{dz'}{\ell} d^2\rho' \frac{d\Omega}{4\pi} \quad (6)$$

where c is the light velocity.

Due to the translational invariance in the x - y plane, P depends on the projection $\boldsymbol{\rho} = (\mathbf{r} - \mathbf{r}')_{\perp}$ on the interface plane and the emerging energy can be therefore given per unit surface. Finally, the total time-dependent albedo is defined as the ratio of the emergent energy per unit surface, unit time and unit solid angle $d\Omega$ to the incident energy flux along the direction \hat{s}_0 :

$$\alpha(\hat{s}_0, \hat{s}, t) = \frac{c}{4\pi\ell^2} \int dz dz' d^2\rho e^{-z/\mu_0 \ell} \times e^{-z'/\mu \ell} \{1 + \cos k(\hat{s} + \hat{s}_0) \cdot (\mathbf{r} - \mathbf{r}')\} \times P(\boldsymbol{\rho}, z, z'; t). \quad (7)$$

In this expression, μ and μ_0 are respectively the projections of \hat{s} and \hat{s}_0 on the z -axis. The factor $\{1 + \cos [k(\hat{s} + \hat{s}_0) \cdot (\mathbf{r} - \mathbf{r}')]\}$ accounts for the interference effects for the ensemble averaged albedo as discussed in the introduction. The exponential factors $e^{-z'/\mu \ell}$ and $e^{-z/\mu_0 \ell}$ account for the damping of the incident and emergent waves. They come from the fact that the intensity which propagates in the medium is not issued directly from the incident source pulse but comes from reduced intensity sources (following the terminology of Ref. [18]). At this point, let us also note that the distance travelled by the waves before the first and after the last scattering events differs for a given sequence and its time reverse counterpart as noted by Tsang and Ishimaru [5]. It gives instead of equation (7) :

$$\alpha(\hat{s}_0, \hat{s}; t) = \frac{c}{4\pi\ell^2} \int dz dz' d^2\rho P(\boldsymbol{\rho}, z, z'; t) \left\{ e^{-\frac{z}{\mu_0 \ell} - \frac{z'}{\mu \ell}} + e^{-\frac{1}{2} \left\{ \frac{1}{\mu_0} + \frac{1}{\mu} \right\} \cdot \frac{z+z'}{\ell}} \cos [k(\hat{s} + \hat{s}_0) \cdot (\mathbf{r} - \mathbf{r}')] \right\}. \quad (8)$$

This expression still gives the factor two right in the backscattering direction. Although important, we will neglect in the remaining calculations of this article the difference between equations (7) and (8) since we are interested by the small angle regime where μ and μ_0 are of order one. Finally, the single scattering contribution in equation (7) has been omitted since it is not justifiable of any interference effect.

The expression (7) has been obtained for a dynamical experiment where an energy pulse is incident on the medium. Defining $P(\rho, z, z')$ as the time-integral of $P(\rho, z, z'; t)$, we can obtain the stationary counterpart of equation (7) as :

$$\alpha(\delta_0, \delta) = \frac{c}{4\pi\ell^2} \int_0^\infty dz \int_0^\infty dz' e^{-z/\mu_0\ell} e^{-z'/\mu\ell} \times \\ \times \int_s d^2\rho [1 + \cos \mathbf{q} \cdot (\mathbf{r} - \mathbf{r}')] P(\rho, z, z') \quad (9)$$

which was established in reference [12]. Except for the interference effect, the calculation of the stationary albedo $\alpha(\delta_0, \delta)$ reduces to that of the function $P(\rho, z, z')$ describing the classical transport intensity.

This problem is well-known as the Schwarzschild-Milne [19] problem first considered to study the flow of light in a stellar atmosphere.

It follows from the radiative transport theory or from more microscopic approaches (see Sect. 3) that $P(\rho, z, z')$ obeys the integral equation :

$$P(\mathbf{r}, \mathbf{r}') = \frac{1}{4\pi\ell} \int d^3r'' \frac{\exp\left(-\frac{|\mathbf{r} - \mathbf{r}''|}{\ell}\right)}{|\mathbf{r} - \mathbf{r}''|^2} P(\mathbf{r}'', \mathbf{r}') \\ + \frac{1}{4\pi c|\mathbf{r} - \mathbf{r}'|^2} \cdot \exp\left(-\frac{|\mathbf{r} - \mathbf{r}'|}{\ell}\right). \quad (10)$$

The insertion of the solution of equation (10) for the half-space problem in equation (9) yields the total stationary albedo. The resulting formula is identical to those derived by Tsang and Ishimaru [5] and Van der Mark *et al.* [22] except for the small difference in the exponential factors between the coherent and incoherent contributions already discussed. To compare the different formulas quantitatively let us note that our function P is related to their ladder intensity F by $P = \frac{\ell^2}{4\pi c} F$. The stationary expression of the albedo represents an improvement compared to its dynamical counterpart. The integral equation determining time-dependent function P is more complicated and the usual method consists in solving it in the diffusion approximation and to deduce P within the same limit. But equation (10) is exact and moreover it must be noted that it can also be solved in the diffusion approximation in an equivalent way.

As shown by the numerical calculations of Van der Mark *et al.* [22] the expansion of the resulting α in successive orders of scattering is, except for the very first orders identical to that found by using the solution of the diffusion equation to be discussed below. This is therefore a justification for using this approximation, which we shall do hereafter in the remaining part of this paper.

Before considering in detail this approximation, let us discuss some problems related to the boundary conditions in connection with equation (10). From it, we can obtain the corresponding integral equation for the so-called mean-density of energy $U(z)$ (which has the dimension of an inverse volume) :

$$U(z) = \int_0^\infty \frac{dz'}{\ell} E_1\left(\frac{|z - z'|}{\ell}\right) U(z') + \\ + \frac{1}{4\pi\ell^3} \int_0^\infty \frac{dz'}{\ell} E_1\left(\frac{|z - z'|}{\ell}\right) \exp\left(-\frac{z'}{\mu_0\ell}\right) \quad (11)$$

where

$$E_1(x) \equiv \int_1^\infty e^{-xt} \frac{dt}{t}. \quad (12)$$

This relation known as the Milne-equation is actually a direct consequence of the conservation of energy. For sources located at the infinity within the medium, the second term of equation (11) is absent and one is dealing with the true Milne problem which has the advantage to be solved exactly for point-like scatterers and no incident flux onto the outer surface $z = 0$ by mean of the Wiener-Hopf method [20]. It gives an energy density profile $U(z)$ which cancels on the plane $z = -z_0$ where $z_0/\ell = 0.7104\dots$. This exact solution will be of great help for the diffusion approximation we consider now.

The important term in equation (6) is the Green's function $P(\mathbf{r}, \mathbf{r}', t)$ which obeys a transport equation in the most general situation. Far enough from the interface, it can be shown that this transport equation can be approximated by a diffusion equation :

$$\left(D \nabla_r^2 + \frac{\partial}{\partial t}\right) P(\mathbf{r}, \mathbf{r}'; t) = \delta(\mathbf{r} - \mathbf{r}') \delta(t) \quad (13)$$

where $D = \frac{1}{d} \ell c$.

It means that for long time and long distance (compared respectively to τ and ℓ), the local light intensity has a diffusive motion in the disordered medium. $P(\mathbf{r}, \mathbf{r}', t)$ is therefore the probability distribution to go from \mathbf{r} to \mathbf{r}' in a time t for a random walk which never crosses the interface. This last condition would be taken into account by cancelling the probability P on the surface at $z = 0$. Nevertheless we know from the exact solution of the Milne problem that P cancels on the plane

$z = -z_0$ with $z_0 = 0.7104... \ell$. On the other hand within the stationary diffusion approximation, the boundary condition consists in cancelling the energy flux flowing towards the disordered medium at $z = 0$. Then the probability P vanishes on the plane $z = -z_0$ where $z_0 = 2/3 \ell$. In the following, we will adopt $z_0 = 2/3 \ell$ which applies as well to the more general situation of time dependent experiments. Within this approximation, one obtains :

$$P(\mathbf{r}, \mathbf{r}', t) = \frac{1}{(4\pi Dt)^{3/2}} e^{-\rho^2/4Dt} \times \\ \times [e^{-(z-z')^2/4Dt} - e^{-(z+z'+2z_0)^2/4Dt}]. \quad (14)$$

In this relation, the translational invariance of the average medium along the x and y directions imposes that P depends only on $\rho = |(\mathbf{r} - \mathbf{r}')_{\perp}|$, while the bracketed terms express the fact that the diffusion paths do not cross the interface plane. The diffusion constant is $D = 1/3 \ell c$ where the renormalization due to weak localization effects is neglected. In three-dimensional systems, it is justified for small enough λ/ℓ .

2.1 THE TIME-DEPENDENT ALBEDO. — The time-dependent albedo $\alpha(\theta, t)$ as defined by equation (7) can be calculated at the same level of approximation [23]. It is the response to an impulsion at time $t = 0$ in a direction defined by the angle θ to the backscattering direction. In this dynamical experiment, different time scales occur describing different physical phenomena. We restrict here the discussion to the case of aqueous suspension of latex microspheres studied in reference [10].

The shortest time scale is given by the transport elastic scattering time τ which is of order of 10^{-13} s.

Another characteristic time scale is provided by

$$\alpha_c(\theta, t) = \frac{c}{4\pi\ell^2} \cdot \frac{1}{2\sqrt{\pi Dt}} \int_0^{\infty} dz dz' e^{-z/\ell} e^{-z'/\ell} \left[\exp\left(-\frac{(z-z')^2}{4Dt}\right) - \exp\left(-\frac{(z+z'+2z_0)^2}{4Dt}\right) \right] \times \\ \times \int d^2\rho e^{i\mathbf{k}_{\perp} \cdot \boldsymbol{\rho}} \frac{1}{4\pi Dt} e^{-\rho^2/4Dt} \quad (15)$$

where $\mathbf{k}_{\perp} = k(\hat{s} + \hat{s}_0)_{\perp}$ and $k_{\perp} \cong \frac{2\pi}{\lambda} \theta$. The angular dependence of $\alpha_c(\theta, t)$ arises only from the last Gaussian integral and the remaining z -integrals act only as weighting factors. In the long time limit $\sqrt{Dt} \gg \ell$ one has :

$$\alpha_c(\theta, t) \cong \frac{(z_0 + \ell)^2}{8\pi^{3/2}} \frac{c}{(Dt)^{3/2}} e^{-Dtk_{\perp}^2} \quad (16)$$

or

$$\alpha_c(\theta, t) \cong \alpha_{\text{inc}}(t) e^{-Dtk_{\perp}^2}. \quad (17)$$

the time τ_B associated with Brownian motion of the scatterers. More precisely, it is defined through $\tau_B = \lambda^2/D_B$ where D_B is the diffusion constant of the Brownian particles. τ_B is of order 10^{-3} s. For time scales smaller than τ_B , the scatterers can be considered immobile and one single spatial configuration of the scatterers is explored for which strong intensity fluctuations (speckle) are expected. Averaged quantities must be obtained practically by the usual averaging over measurements. For time scales larger than τ_B , the Brownian motion of the scatterers could provide coarse-grained self-averaging quantities.

A third time scale arises from the breaking of time reversal invariance due to the Brownian motion of the scatterers. This situation has been carefully analysed by Golubentsev [8]. Let us consider a multiple scattering sequence of length $L = N\ell$. The travel time of light through this sequence is $t = N\tau$. If during the time t , the scatterers moved over a total length larger than λ , then the phase-coherence between the two time-reversed paths breaks down and the interference effect disappears.

During a time t , each scatterer moves by diffusion over a distance $\sqrt{\Delta r^2} \cong \sqrt{D_B t}$. Then, the N scatterers move over a total distance such that $L^2 = N \Delta r^2 = N D_B t$. To observe the interference effect between time-reversed sequences, we must have $L < \lambda$. The coherent backscattering phenomenon will therefore be observable for times $t < \lambda^2/N D_B$, or $t < \sqrt{\tau \tau_B}$. This is the third characteristic time scale associated with the breaking of time reversal invariance. Let us now compute the angular lineshape of the coherent albedo for $t \ll \sqrt{\tau \tau_B}$. For convenience in the calculations, let us consider the case of normal incidence ($\mu_0 = 1$) and quasi-normal emergence ($\mu \cong 1$). We can therefore write the coherent part of the albedo as :

These expressions show that :

a) at a given time t , the reflected echo is enhanced by a factor $(1 + e^{-Dtk_{\perp}^2})$ within a cone of angular width $\theta_c = \lambda/2\pi\sqrt{Dt}$. It is a consequence of the fact that the typical size of diffusion paths is \sqrt{Dt} ,

b) the amplitude $\alpha_{\text{inc}}(t)$ of the incoherent part of the echo is proportional to the probability for a random walk to cross the plane $z = -z_0$ after a time t and decreases like $t^{-3/2}$. This result is actually valid

at any space dimensionality and especially in 2 dimensions where the last part of (15) must be changed into $\int d\rho \frac{1}{\sqrt{Dt}} e^{-\rho^2/4Dt}$ which leaves the time dependence of (16) unchanged,

c) for a fixed value of the angle θ_0 , the coherent albedo decreases as $(\tau/t)^{3/2}$ for times $t \ll t_c(\theta_0)$ where $t_c(\theta_0) = \frac{\lambda^2}{4\pi^2 D \theta_0^2}$ while for times $t \gg t_c(\theta_0)$, it is exponentially damped as expected $\alpha_c(\theta_0, t) \propto \frac{e^{-t/t_c(\theta_0)}}{t^{3/2}}$.

Let us now summarize the time-dependent effects as shown in figure 3. At a given angle θ_0 , we observe the average intensity reflected by the disordered medium. Suppose that θ_0 is large enough such that

$$t_c(\theta_0) < \sqrt{\tau\tau_B}, \quad \text{i.e.} \quad \theta_0 > \frac{\lambda}{2\pi\ell} \left(\frac{\tau}{\tau_B} \right)^{1/4}$$

(which is of order of $3 \times 10^{-3} \frac{\lambda}{2\pi\ell}$). Then at times t between τ and $t_c(\theta_0)$ the reflected intensity is enhanced by nearly a factor of two, and decreases in the same way as the incoherent part of the echo like $(\tau/t)^{3/2}$. It converges to the incoherent value as an exponential around $t_c(\theta_0)$, due to the lack of coherence between time-reversed paths of length larger than $3\lambda^2/4\pi^2\theta_0^2\ell$.

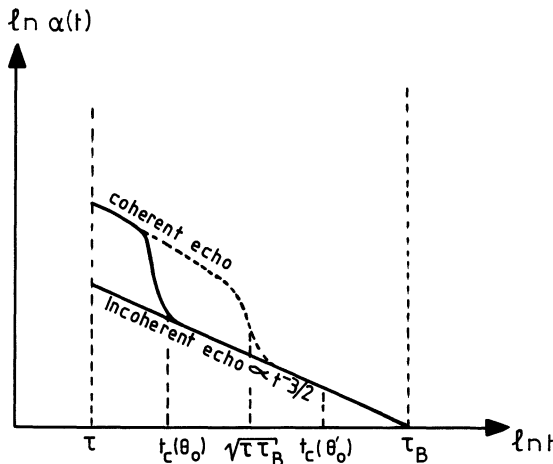


Fig. 3. — Time-dependent albedo.

Suppose now that θ_0 is smaller than $\frac{\lambda}{2\pi\ell} \left(\frac{\tau}{\tau_B} \right)^{1/4}$ i.e. $t_c(\theta_0) > \sqrt{\tau\tau_B}$. Then at times t between τ and $\sqrt{\tau\tau_B}$, we observe the coherent backscattering echo in the same way as previously, while it converges to the incoherent values around

$\sqrt{\tau\tau_B}$ due now to the breaking of time-reversal invariance by the Brownian motion of the scatterers.

Let us discuss now the possibility of observation of the coherent dynamical echo.

First of all, for aqueous suspension of latex microspheres, the characteristic values of τ and τ_B given above imply that $\sqrt{\tau\tau_B} \approx 10^{-8}$ s. Therefore, the resolution time of a dynamical experiment should be at least of the order of the nanosecond. Such a resolution has been achieved recently [29] in order to measure the transmission coefficient of disordered systems. For such a nanosecond resolution, the coherent echo will be observed only if $t_c(\theta_0) \geq 1$ ns, i.e. $\theta_0 \leq 3 \times 10^{-3} \lambda/\ell$ for suspensions considered above. According to the experimental results of reference [10], where $\lambda/2\pi\ell \approx 3 \times 10^{-3}$ rd, we need an angular resolution better than $10 \mu\text{rd}$. Until now the best angular resolution has been obtained by Kaveh *et al.* [17] and is $\sim 50 \mu\text{rd}$. Then, the measure of the dynamical albedo requires another system in which the transport mean free time τ is decreased such as in random distribution of submicron titania crystals recently considered by Genack [26].

2.2 STATIONARY ALBEDO. — We now evaluate the albedo for a stationary incident flux, which corresponds to the experimental situation described in reference [10]. According to the general equation (7) we have to integrate over time the expression (15) in order to obtain the coherent part of the stationary albedo. This is easily done using a Fourier transform of $P(\mathbf{r}, t)$. Then the expression of $\alpha_c(\theta)$ is

$$\alpha_c(\theta) = \frac{3}{8\pi} \cdot \mu\mu_0 \cdot \frac{1}{(1 + \mu k_\perp \ell)(1 + \mu_0 k_\perp \ell)} \times \left(\frac{1 - e^{-2k_\perp z_0}}{k_\perp \ell} + 2 \frac{\mu\mu_0}{\mu + \mu_0} \right). \quad (18)$$

Within the small angle limit ($\mu \approx \mu_0$) and for normal incidence $\mu \approx \mu_0 \approx 1$, we have :

$$\alpha(\theta) = \frac{3}{8\pi} \left[1 + \frac{2z_0}{\ell} + \frac{1}{(1 + k_\perp \ell)^2} \times \left(1 + \frac{1 - e^{-2k_\perp z_0}}{k_\perp \ell} \right) \right]. \quad (19)$$

This expression exhibits two interesting features : the angular width inside which the coherent effect is observable is of order $\lambda/2\pi\ell$ as expected and near the exact backscattering direction, the albedo varies linearly with angle θ :

$$\alpha_c(\theta) \approx \alpha_{\text{inc}} \left(1 - 2 \frac{(\ell + z_0)^2}{\ell + 2z_0} k_\perp + O(k_\perp^2) \right) \quad (20)$$

$$\approx \alpha_{\text{inc}} - \frac{3}{4\pi} \frac{(\ell + z_0)^2}{\ell} k_{\perp} + O(k_{\perp}^2). \quad (21)$$

Hence the lineshape of the coherent backscattering peak is triangular. Such a singularity originates from the fact that, at $\theta = 0$, the coherent contribution of all diffusion paths produces an infinite sum of Gaussian terms. Although each term is parabolic near $\theta = 0$, their sum gives rise to a triangular singularity. Alternatively, the coherent contribution to the albedo can also be considered [12] as a « structure factor » of the stationary transport term $\int_{\tau}^{\infty} dt P(\mathbf{r}, \mathbf{r}'; t)$. The variable θ probes the size of the diffusion paths in the medium. The smaller the angle θ , the larger the maximal size of the loops, which means that, at a given angle θ , only the paths of length L smaller than $\lambda^2/\ell\theta^2$ contribute to the coherent albedo. Hence, the quantity $\lambda^2/D\theta^2$ is analogous to the phase coherence time τ_{ϕ} first introduced by Larkin and Khmel'nitskii [21]. For electronic systems, τ_{ϕ} is identified with the temperature-dependent inelastic scattering time $\tau_i \propto T^{-p}$ (where p is some positive exponent). Then, the contribution of diffusion paths at $\theta = 0$ corresponds to the ideal situation where the temperature would be exactly zero in electronic systems and the phase coherence time infinite. Actually, in real systems the absorption of light represents a mechanism which prevents the observation of this coherence close to $\theta = 0$ as developed in the following part.

2.3 EFFECTS OF ABSORPTION AND FREQUENCY. — Consider an incident light whose intensity is modulated at frequency Ω . If the incident intensity is of the form $I(t) = I_0 e^{i\Omega t}$, the modulated part of the signal at frequency Ω is proportional to [23]:

$$\alpha(\theta, \Omega) = \frac{1}{4\pi\ell\tau} \int dz dz' d^2\rho e^{-z/\mu_0\ell} e^{-z'/\mu\ell} \times \\ \times (1 + \cos(\mathbf{k}_{\perp} \cdot \boldsymbol{\rho})) P(\mathbf{r}, \mathbf{r}'; \Omega) \quad (22)$$

where $P(\mathbf{r}, \mathbf{r}'; \Omega)$ is obtained from equation (14) by a time Fourier transform. Let us note at this stage that the interference factor $\cos(\mathbf{k}_{\perp} \cdot \boldsymbol{\rho})$ is purely geometrical and therefore is not affected by the Fourier transform. This calculation leads to an expression of $\alpha(\theta, \Omega)$ deduced from $\alpha(\theta, \Omega = 0)$ by the formal replacement $k_{\perp}^2 \leftrightarrow k_{\perp}^2 - i\Omega/D \equiv k_{\perp}^2 - i\xi^{-2}$ so that

$$\alpha_c(\theta, \Omega) = \alpha_c(k_{\perp}, \xi) = \alpha_c(k_{\perp}^2 - i\xi^{-2}, 0).$$

The new characteristic length $\xi = \sqrt{D/\Omega}$ is the diffusion length at the frequency Ω . In the asymptotic limit $k_{\perp}\xi \gg 1$, the modulated coherent response is identical to its stationary counterpart, i.e. $\alpha_c(k_{\perp}, \xi) \approx \alpha_c(k_{\perp})$. But in the limit $k_{\perp}\xi \ll 1$, the

modulus of the coherent albedo reduces to:

$$|\alpha_c(\theta, \Omega)| = \frac{3}{8\pi\ell} \left[(\ell + 2z_0) - \frac{\sqrt{2}}{\xi} (z_0 + \ell)^2 - \frac{(z_0 + \ell)^2}{\xi\sqrt{2}} (k_{\perp}\xi)^2 + O(k_{\perp}\xi)^4 \right]. \quad (23)$$

Therefore, $\alpha_c(0, \Omega)$ is smaller than $\alpha_c(0, 0)$ by a quantity of order ℓ/ξ . The physical meaning of this reduction is as follows: the modulation of the incident light is washed out for loops of length $L \geq c/\Omega$, i.e. of transverse extension larger than ξ . Nevertheless, it must be noted that we still obtain the enhancement factor 2, i.e. $\alpha_c(0, \Omega) = \alpha_{\text{inc}}(0, \Omega)$. At this point, a comparison with the effect of thermal motion of the scatterers and with the electronic case appears to be useful. In these cases, the ratio between α_c and α_{inc} is smaller than one. For weakly localized electronic systems, the role of the inelastic scattering is to break the time reversal invariance between diffusion paths of extension larger than $\sqrt{\tau_i/\tau}$ leaving unchanged the incoherent contribution to the classical transport coefficient. Then, τ_i for electrons has exactly the same effect as τ_B for the light. But, in contrast, for the case of light, the role of the frequency (or absorption as we shall see) is to decrease in the same way both the coherent and incoherent contributions to the albedo. This leaves unchanged the factor of two in the backscattering direction.

Let us now consider the effect of absorption [23]. The presence of absorption in the disordered medium can be described by a characteristic time $\tau_a = \ell_a/c$ where ℓ_a is the absorption length. The total albedo can now be obtained by the simple relation:

$$\alpha_{\text{abs}} = \int_0^{\infty} dt \alpha(t) e^{-t/\tau_a} \quad (24)$$

where $\alpha(t)$ is the time-dependent albedo. Within the diffusion approximation, $\alpha_{\text{abs}}(\theta, \tau_a)$ can be obtained in the same way as for the frequency dependent albedo, from the stationary non-absorbing case by mean of the formal replacement of k_{\perp} by $(k_{\perp}^2 + k_a^2)^{1/2}$:

$$\alpha_{\text{abs}}(k_{\perp}, k_a) = \alpha_c((k_{\perp}^2 + k_a^2)^{1/2}, 0) \quad (25)$$

where $k_a^{-1} = \sqrt{D\tau_a} = \sqrt{\frac{\ell\ell_a}{3}}$ and $k_{\perp} = \frac{2\pi\theta}{\lambda}$ as usual. In the backscattering direction we obtain:

$$\alpha_{\text{abs}}(0, k_a) = \alpha_c(k_a, 0). \quad (26)$$

The validity of this relation has been recently demonstrated experimentally [10]. As mentioned above, the absorption acts only to decrease equally both coherent and incoherent contributions to the

albedo. The transformation of the linear regime at small angles, $\theta < \lambda/2\pi \sqrt{\ell\ell_a}$, into a parabolic one can therefore be simply understood as the elimination of all the scattering sequences of lengths larger than the absorption length ℓ_a .

2.4 THE ALBEDO FROM TRANSPORT THEORY: THE PROBLEM OF ANISOTROPIC SCATTERING. — Up to now, we have only considered the case of isotropic scattering. However, for finite size scatterers, it is not isotropic. The diffusion constant D is then given by $D = c\ell^*/3$, where ℓ^* is the transport mean free path defined by :

$$\frac{1}{\ell^*} = n \int_0^\pi \sigma(\omega)(1 - \cos \omega) d\omega \quad (27)$$

where n is the density of the uncorrelated scatterers and $\sigma(\omega)$ the differential cross-section. For scatterers of large size compared to the wavelength, the scattering is mainly in the forward direction and the ratio between ℓ^* and ℓ can easily be ten in practical cases [10]. As ℓ^* and not ℓ enters the diffusion constant D , it can be expected that at least at small angles, the lineshape should involve ℓ^* rather than ℓ . The aim of this part is to give a short derivation of this fact. Equation (7) is of little help because it is not clear where ℓ should be replaced by ℓ^* in the damping factors $\frac{e^{-z/\mu\ell}}{\ell}$. It is thus simpler to use transport theory. For the sake of concision we shall use the same notation and follow the derivation of the diffusion equation of chapter 7 of reference [18]. Let us define $U_d(\mathbf{r})$ as the local diffuse energy density at point \mathbf{r} . By assuming a smooth variation of $U_d(\mathbf{r})$ on the length scale of ℓ , it can be shown that $U_d(\mathbf{r})$ obeys a diffusion equation which is written in the particular case of an interface illuminated by a point source $F_0(\boldsymbol{\rho}) = F_0 \delta_2(\boldsymbol{\rho})$:

$$\nabla^2 U_d(\mathbf{r}) = -\frac{3}{4\pi} \frac{1}{\ell^2} F_0(\boldsymbol{\rho}) e^{-z/\mu_0\ell} \quad (28)$$

with the following boundary condition at the interface :

$$U_d(z=0) - z_0 \left(\frac{\partial U_d}{\partial z} \right)_{z=0} + \frac{Q_1(0)}{2\pi} = 0 \quad (29)$$

where z_0 has the value $2/3 \ell^*$.

This relation must be satisfied at any point ρ of the interface ; it expresses the property that the flux of diffuse intensity towards the medium vanishes at the interface. $Q_1(0)$ represents the effect of anisotropy of the scattering pattern and vanishes for isotropic scatterers. It depends on the transport mean free path ℓ^* by the relation :

$$Q_1(0) = \left(\frac{\ell^*}{\ell} - 1 \right) F_0(\boldsymbol{\rho}). \quad (30)$$

We recall that the boundary condition (29) is only approximate. By comparing this relation to the exact boundary condition for the special case of isotropic scatterers, the value of z_0 changes weakly from $2/3 \ell^*$ to $0,7104 \ell^*$ but we will neglect this difference here. In the problem of the albedo, we are interested in the energy density $U_d(\boldsymbol{\rho}, 0)$ at the interface $z = 0$. This solution of equations (28) and (29) can be obtained by a Bessel transform which gives :

$$U_d(\rho, z=0) = \frac{F_0 \ell^*}{\ell 4\pi^2} \int_0^\infty d\lambda \times \\ \times J_0(\lambda\rho) \frac{\lambda}{1 + \frac{2}{3} \ell^* \lambda} \left[\frac{1}{1 + \lambda\ell} - \beta \right] \quad (31)$$

where $J_0(\lambda\rho)$ is the zero order Bessel function and β the correction of anisotropy for the mean free path :

$$\beta = 1 - \ell/\ell^*.$$

The emerging flux at ρ is $\frac{5}{2} U_d(\rho, z=0)$ [18].

Hence, from $U_d(\rho, z=0)$, we calculate the total albedo (coherent part) by the two-dimensional Fourier transform of $U_d(\rho, 0)$:

$$\alpha_c(\theta) = \frac{5}{2} \int_s U_d(\rho, 0) e^{i\mathbf{k}\boldsymbol{\rho}} d^2\rho \quad (33)$$

where the integral is on the interface plane. It finally gives :

$$\alpha_c(\theta) \approx \frac{5}{4\pi} \cdot \frac{1}{1-\beta} \frac{1}{\frac{2}{3} \ell^* k_\perp + 1} \left(\frac{1}{1 + \ell k_\perp} - \beta \right) \quad (34)$$

which in the small angle regime ($k_\perp \ell \ll 1$) reduces to :

$$\alpha_c(\theta) \approx \alpha_c(0) - \frac{25}{12\pi} k_\perp \ell^*. \quad (35)$$

We note that the value of $\alpha_{\text{inc}} = \alpha_c(0)$ does not depend on the ratio ℓ^*/ℓ . This is implied by the definition of the boundary condition for the diffusion approximation. But α_{inc} differs from that found by the image method. This is not surprising since this value depends on the weight of small paths, which are differently described in the two approaches.

In contrast, the absolute slope given by equation (35) is identical to that obtained for isotropic scatterers by the image method (cf. Eq. (21) with $z_0 = \frac{2}{3} \ell$) if one replaces everywhere the elastic mean free path by the transport mean free path ℓ^* . This is physically appealing since one expects the absolute slope of the coherent albedo to depend only on the contribution of long light paths and not on the detailed exponential factors near the interface ($e^{-z/\ell}$ and $e^{-z'/\ell}$) for the incident and emergent waves. Ultimately it comes from the diffusion theory

and hence depends only on $D = 1/3 \ell^* c$. This result can be seen as a justification of the formal replacement of ℓ by ℓ^* in equation (21). On the other hand, this expression of $\alpha_c(\theta)$ given by the transport theory becomes incorrect for $k_\perp \ell^*$ large enough since then the total albedo becomes negative. This unphysical result is the consequence of the well-known fact that the diffusion approximation (cf. Eq. (28)) is only valid on length scales larger than ℓ^* . It is not critical in the isotropic regime, since in this case $\beta = 0$ and the albedo never becomes negative.

3. Microscopic derivation for the expression of the albedo.

In the previous section, we have established a heuristic expression of the albedo $\alpha(\theta)$ based on two basic ingredients. First, the coherent effect due to time reversal symmetry provides the phase factor ; i.e. the angular variation of the albedo. Secondly, the intensity transport in the bulk was obtained in the asymptotic limit of long-times as the solution of a diffusion equation whose boundary conditions for the semi-infinite geometry are accounted for by the image method.

Our aim now is to recover these results starting from the elementary collisions experienced by an incident plane wave. This program will be carried out in two distinct steps. The first one consists to establish the existence and the form of the interference term appearing in equation (4) in its full generality from microscopic arguments. We shall see that this form in equation (4) where Q represents the incoherent contribution to the intensity transport is actually valid in a bulk. The second step is devoted to the study of the expression of the albedo of a semi-infinite medium. In such a medium, the coherent term remains in force, but it appears under a slightly modified form as shown by Tsang and Ishimaru [5]. It must be noted here that this modification as well as the final expression of $\alpha(\delta, \delta_0)$ are based on various approximations which give to this derivation less generality than the argument developed in the first step.

Let us now specify these points. For the sake of simplicity, we will consider here the scalar case for which the electromagnetic field has only one component.

The retarded Green function for the wave amplitude $A(r)$ is defined as the solution of the equation :

$$[\nabla_r^2 + k_0^2(1 + n(\mathbf{r})) + i\eta] G(\omega, \mathbf{r}, \mathbf{r}_0) = \delta(\mathbf{r} - \mathbf{r}_0) \quad (36)$$

where $k_0 = \frac{2\pi}{\lambda_0}$ with λ_0 the wavelength in free space, while $n(\mathbf{r})$ represents the fluctuating part of the refractive index giving rise to the multiple

scattering. Finally, ω is the frequency of the incident wave such that $\omega = ck$ (c being the light velocity in the medium).

The Green function G is related to the amplitude $A(\mathbf{r})$ of the wave in a point r by

$$A(\mathbf{r}) = \int_v d^d r' G(\omega, \mathbf{r}, \mathbf{r}') S(\mathbf{r}') \quad (37)$$

where $S(\mathbf{r}')$ is the source function.

In free space, i.e. without scattering centres ($n(\mathbf{r}) = 0$), the solution of equation (36) is given by :

$$G_0(\mathbf{r}, \mathbf{r}_0, \omega) = \frac{e^{ik_0|\mathbf{r}-\mathbf{r}_0|}}{4\pi|\mathbf{r}-\mathbf{r}_0|} \quad (38)$$

When $n(\mathbf{r})$ is different from zero, the wave is scattered many times and this scattering can be described by the S -matrix or equivalently the mass operator M through the Dyson equation for the average propagator

$$\bar{G}(\mathbf{r}, \mathbf{r}_0, \omega) = G_0(\mathbf{r}, \mathbf{r}_0, \omega) + \int G_0(\mathbf{r}, \mathbf{r}_1, \omega) \times \\ \times M(\mathbf{r}_1, \mathbf{r}_2) \bar{G}(\mathbf{r}_2, \mathbf{r}_0, \omega) d\mathbf{r}_1 d\mathbf{r}_2 \quad (39)$$

or in an operator form :

$$\bar{G} = G_0 + G_0 M \bar{G} \quad (40)$$

The mass operator M renormalizes the free propagator G_0 . It can be calculated by standard diagrammatic expansion (see Appendix A) and one obtains :

$$\bar{G}(\mathbf{r} - \mathbf{r}_0, \omega) = \frac{1}{4\pi|\mathbf{r} - \mathbf{r}_0|} e^{ik_{\text{eff}}|\mathbf{r} - \mathbf{r}_0|} \quad (41)$$

where $k_{\text{eff}} = k - M(k)/2k$. The elastic mean free path or extinction length $\ell(\omega)$ is therefore defined by $\ell^{-1}(\omega) = -\text{Im} M(k)/k$. This expression gives for example the well-known Rayleigh expression in the limit of low density of point-like scatterers and low frequency. It must be noted here that equation (39) (or (40)) is by no way a transport equation, and therefore $\ell(\omega)$ is not the transport mean free path but the extinction length only describing the scattering properties of the averaged disordered medium.

Let us now turn to the intensity propagation through the disordered medium. In order to describe the transport properties we need to calculate the correlation function of the propagators defined by :

$$G_2(\mathbf{r}_1, \mathbf{r}'_1; \mathbf{r}_2, \mathbf{r}'_2) = \overline{G(\mathbf{r}_1, \mathbf{r}'_1) G^*(\mathbf{r}_2, \mathbf{r}'_2)} \quad (42)$$

where G^* is the complex conjugate of G . As before, this correlation functions obeys an equation of motion, the Bethe-Salpeter equation given by :

$$G_2 = \bar{G}\bar{G}^* + \bar{G}\bar{G}^* U G_2 \quad (43)$$

in an operator form. The operator U which renormalizes G_2 can also be calculated by a standard diagrammatic expansion as shown below. The Bethe-Salpeter equation is the equivalent (at a microscopic level) of the Boltzmann or radiative transfer equation used in phenomenological approaches. In this equation U represents the sum of all the diagrams obtained from the interaction of the wave with the scatterers. For the sake of clarity let us describe the double scattering situation for the propagation of incoherent intensity. It is given by :

$$\int d^3r \int d^3r' \bar{G}(\omega, \mathbf{r}_1 - \mathbf{r}) \bar{G}^*(\omega, \mathbf{r}_2 - \mathbf{r}) \times \\ \times \Gamma(k\hat{s}_{r_1 r}, k\hat{s}_{r r'}; k\hat{s}_{r_2 r}, k\hat{s}_{r r'}) \\ \times \bar{G}(\mathbf{r} - \mathbf{r}', \omega) \bar{G}^*(\omega, \mathbf{r} - \mathbf{r}') \\ \times \Gamma(k\hat{s}_{r r}, k\hat{s}_{r' r_1}; k\hat{s}_{r r'}, k\hat{s}_{r' r_2}) \\ \times \bar{G}(\omega, \mathbf{r}' - \mathbf{r}'_1) \bar{G}^*(\omega, \mathbf{r}' - \mathbf{r}'_2) \quad (44)$$

where the function $\Gamma(s_1, s_2; s'_1, s'_2)$ describes the scattering process for the function G and G^* from the directions \hat{s}_1 and \hat{s}_2 towards the directions \hat{s}'_1 and \hat{s}'_2 respectively. The expression given by equation (44) is obtained within the Fraunhofer limit, and the propagators \bar{G} and \bar{G}^* between two collisions are uncorrelated. In order to simplify equation (44), let us introduce the quantities :

$$F_0(\mathbf{r}, \hat{s}; \mathbf{r}', \hat{s}') = \bar{G}(\omega, \mathbf{r} - \mathbf{r}') \bar{G}^*(\omega, \mathbf{r} - \mathbf{r}') \times \\ \times \delta(\hat{s} - \hat{s}') \delta\left(\hat{s} - \frac{\mathbf{r} - \mathbf{r}'}{|\mathbf{r} - \mathbf{r}'|}\right) \quad (45)$$

$$\tilde{F}_0(\mathbf{r}_1, \mathbf{r}_2, \mathbf{r}_3) = \bar{G}(\omega, \mathbf{r}_1 - \mathbf{r}_3) \bar{G}^*(\omega, \mathbf{r}_2 - \mathbf{r}_3)$$

and

$$T(\mathbf{r}, \hat{s}; \mathbf{r}', \hat{s}') = \delta(r - r') \Gamma(k\hat{s}, k\hat{s}'; k\hat{s}, k\hat{s}'). \quad (46)$$

Then we rewrite equation (44) : $\tilde{F}_0 T F_0 T \tilde{F}_0$. Similarly the propagator $G_2^{(2)}$ of the incoherent correlation function becomes :

$$G_2^{(2)} = G_2^{(s)} + \tilde{F}_0 T \tilde{F}_0 + \tilde{F}_0 T F_0 T \tilde{F}_0 + \dots \quad (47)$$

where the first term $G_2^{(s)}$ represents the free propagation of the intensity in the average medium. The point-like scattering arises in the expansion through the T 's which takes into account all the reducible diagrams. U in equation (43) is the sum of all the diagrams describing all possible scatterings at any order. Two different groups of diagrams contribute to U . The first U_R is the sum of all the reducible diagrams. They are such that if one cuts two propagator lines, one generates two diagrams belonging to U . The second U_i is the sum of all the other diagrams which are irreducible. In U_R , the

dominant contribution comes from the ladder diagrams (contributing to the order zero in λ/ℓ) represented in figure 4a. The dominant contribution in U_i is given, to first order in λ/ℓ , by the so-called maximally crossed diagrams first introduced by Langer and Neal [27] and shown in figure 4b. They can be resummed exactly (cf. Fig. 6) as the sum of a geometric series in the Fourier space. The Fourier transform $U_i(\mathbf{k}, \mathbf{k}'; \Omega)$ of $U_i(\mathbf{r}, \mathbf{r}', t)$ in the bulk is given by (cf. Appendix B) :

$$U_i(k, k'; \Omega) = \frac{b^2 I(\omega, \Omega, q)}{1 - bI(\omega, \Omega, q)} \quad (48)$$

where

$$I(\omega, \Omega, \mathbf{q}) = \sum_{\mathbf{k}} \bar{G}(\mathbf{k}, \omega) \bar{G}^*(-\mathbf{k} + \mathbf{q}, \omega + \Omega),$$

while $b = n_i \sigma / 4 \pi$ where σ is the scattering cross section and n_i the density of the scattering centres. In the limit of small momentum transfer $|\mathbf{k} + \mathbf{k}'| \ell(\omega) \ll 1$ and long time $\Omega \tau(\omega) \ll 1$, we obtain by perturbation expansion :

$$1 - bI(\omega, \Omega, \mathbf{q}) \cong \left(-i\Omega\tau + \frac{\ell^2 q^2}{3} \right) \quad (49)$$

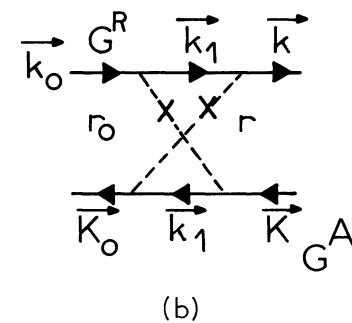
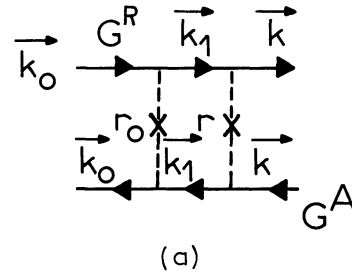


Fig. 4. — (a) Ladder diagram contributing to the order zero in λ/ℓ ; (b) Crossed diagram contributing to first order in λ/ℓ .

$$\begin{array}{c} \vec{P} \\ \vec{Q} \end{array} \begin{array}{c} \vec{P}' \\ \vec{Q}' \end{array} = \frac{1}{2} \left[\begin{array}{c} \vec{P} \\ \vec{Q} \end{array} \begin{array}{c} \vec{P}' \\ \vec{Q}' \end{array} + \begin{array}{c} \vec{P}' \\ \vec{Q}' \end{array} \begin{array}{c} \vec{P} \\ \vec{Q} \end{array} \right]$$

Fig. 5. — Identity relation for crossed diagrams in terms of ladder diagrams.

so that

$$U_i(\mathbf{q}, \omega, \Omega) = \frac{1}{4\pi\ell\tau} \cdot \frac{1}{-i\Omega + D_0 q^2} \quad (50)$$

Therefore, in the hydrodynamic regime $q\ell \ll 1$ and $\Omega\tau \ll 1$, $U_i(\mathbf{q}, \omega, \Omega)$ has a diffusion pole which is at the origin of the diffusion-like motion of the intensity in the disordered medium.

Consider now the Fourier transform of $G_2(\mathbf{r}_1, \mathbf{r}'_1; \mathbf{r}_2, \mathbf{r}'_2)$:

$$\begin{aligned} \tilde{G}_2(\mathbf{k}_1, \mathbf{k}'_1; \mathbf{k}_2; \mathbf{k}'_2) &= \int d^3r_1 d^3r_2 d^3r'_1 d^3r'_2 \times \\ &\times \exp[i(-\mathbf{k}_1 \mathbf{r}_1 + \mathbf{k}_2 \mathbf{r}_2 + \mathbf{k}'_1 \mathbf{r}'_1 - \mathbf{k}'_2 \mathbf{r}'_2)] \\ &\times G_2(\mathbf{r}_1, \mathbf{r}'_1; \mathbf{r}_2; \mathbf{r}'_2) \end{aligned} \quad (51)$$

Let us specify in \tilde{G}_2 the incident and emergent directions:

$$\mathbf{k}_1 = \mathbf{k}_2 = k_0 \hat{s}_i \quad \text{and} \quad \mathbf{k}'_1 = \mathbf{k}'_2 = k_0 \hat{s}_c.$$

We then define

$$g_2^{(L)}(\hat{s}_i, \hat{s}_c) \equiv \tilde{G}_2^{(L)}(k_0 \hat{s}_i, k_0 \hat{s}_c; k_0 \hat{s}_i, k_0 \hat{s}_c) \quad (52)$$

where $G_2^{(L)}$ obeys equation (43) with the reducible diagrams U_R . Knowing that the Fourier transform \mathcal{A} of any given four-points function $A(\mathbf{r}_1, \mathbf{r}_2; \mathbf{r}'_1, \mathbf{r}'_2)$ can be related to the function \hat{A} defined in the reference frame of the centre of mass:

$$\begin{aligned} \mathcal{A}(\mathbf{p}, \mathbf{p}'; \mathbf{q}, \mathbf{q}') &= \int d^3r \int d^3r' \times \\ &\times e^{-i(\mathbf{p}-\mathbf{q})\cdot\mathbf{r}} e^{i(\mathbf{p}'-\mathbf{q}')\cdot\mathbf{r}'} \\ &\times \hat{A}\left(\mathbf{r}, \frac{\mathbf{p}+\mathbf{q}}{2}; \mathbf{r}', \frac{\mathbf{p}+\mathbf{q}'}{2}\right) \end{aligned} \quad (53)$$

and

$$\begin{aligned} g_2^{(c)}(\hat{s}_i, \hat{s}_c) &= \frac{1}{2} \left[\int d^3r \int d^3r' e^{-ik(\hat{s}_i+\hat{s}_c)\cdot\mathbf{r}} e^{ik(\hat{s}_i+\hat{s}_c)\cdot\mathbf{r}'} \hat{G}_2^{(L)}\left(\mathbf{r}, \frac{1}{2}(\hat{s}_c-\hat{s}_i); \mathbf{r}', \frac{1}{2}(\hat{s}_i-\hat{s}_c)\right) + \int d^3r \int d^3r' \right. \\ &\times \left. e^{-ik(\hat{s}_i+\hat{s}_c)\cdot\mathbf{r}} e^{-ik(\hat{s}_i+\hat{s}_c)\cdot\mathbf{r}'} \hat{G}_2^{(L)}\left(\mathbf{r}, \frac{1}{2}(\hat{s}_c-\hat{s}_i); \mathbf{r}', \frac{1}{2}(\hat{s}_i-\hat{s}_c)\right) \right]. \end{aligned} \quad (56)$$

Let \mathbf{q} be the transfer wavevector, $\mathbf{q} = k\mathbf{s}_1$, where $\mathbf{s}_1 = \hat{s}_i + \hat{s}_c$. Then, we have:

$$g^{(c)}(\hat{s}_i, \hat{s}_c) = \int d^3r \int d^3r' \cos\{\mathbf{q}\cdot(\mathbf{r}-\mathbf{r}')\} \hat{G}_2^{(L)}(\mathbf{r}, \hat{s}_c; \mathbf{r}', \hat{s}_i). \quad (57)$$

Finally, for the complete function $g_2(\hat{s}_i, \hat{s}_c)$, we obtain:

$$g_2(\hat{s}_i, \hat{s}_c) = \int d^3r \int d^3r' \{1 + \cos(\mathbf{q}\cdot(\mathbf{r}-\mathbf{r}'))\} \hat{G}_2^{(L)}(\mathbf{r}, \hat{s}_c; \mathbf{r}', \hat{s}_i). \quad (58)$$

At this stage, it must be noted that the sum of the irreducible diagrams, i.e. the first order correction in

where $\mathbf{r} = \frac{\mathbf{r}_1 + \mathbf{r}_2}{2}$ and $\mathbf{r}' = \frac{\mathbf{r}'_1 + \mathbf{r}'_2}{2}$ are the coordinates of the centres of mass, we can write for the function $g_2^{(L)}$:

$$g_2^{(L)}(\hat{s}_i, \hat{s}_c) = \int d^3r \int d^3r' \hat{G}_2^{(L)}(r, \hat{s}_i; r', \hat{s}_c) \quad (54)$$

where $\hat{G}_2^{(L)}$ is related to the Fourier transform \tilde{G}_2 by equation (53).

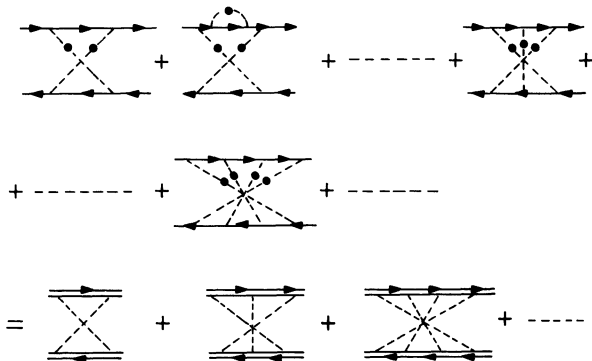


Fig. 6. — Resummation of the crossed diagrams. The simple lines \rightarrow represent the free propagator and the double lines \Rightarrow the renormalized propagator.

Let us now use the time reversal invariance to express at each order of the multiple scattering expansion the equality represented in figure 5, between ladder and maximally crossed diagrams. We then obtain:

$$\begin{aligned} g_2^{(c)}(\hat{s}_i, \hat{s}_c) &= \frac{1}{2} [\tilde{G}_2^{(L)}(k\hat{s}_c, k\hat{s}_i, -k\hat{s}_i, -k\hat{s}_c) \\ &+ \tilde{G}_2^{(L)}(-k\hat{s}_i, -k\hat{s}_c; k\hat{s}_c, k\hat{s}_i)] \end{aligned} \quad (55)$$

λ/ℓ has been completely taken into account and reduces to an interference term, $\cos(\mathbf{q}\cdot(\mathbf{r}-\mathbf{r}'))$.

From this point on, all the quantities will be calculated by the usual *incoherent transport theory*, involving only the expression of $\hat{G}_2^{(L)}(\mathbf{r}, \hat{s}_c; \mathbf{r}', \hat{s}_i)$.

4. Angular dependence of the intensity reflected from a semi-infinite disordered medium.

Up to now, all the quantities we defined are in an infinite medium. Let us consider the case of a semi-infinite medium as represented in figure 2. The albedo of such a medium has been previously defined as the reflected intensity in the direction of observation \hat{s}_c (per unit solid angle), divided by the incident flux F_0 and the sample area S . It is thus related to the intensity $I(\mathbf{R})$ at the point of observation \mathbf{R} in the far field region by $\alpha(\hat{s}_c) = R^2 I(\mathbf{R})/F_0 S$. $I(\mathbf{R})$ is obtained from the average over all possible scattering diagrams with the scattering centres in a half space. This gives [5]:

$$I(\mathbf{R}) = F_0 \int \bar{G}(\mathbf{r}'_1, \mathbf{R}) \bar{G}^*(\mathbf{r}'_2, \mathbf{R}) \tilde{U}(\mathbf{r}_1, \mathbf{r}'_1, \mathbf{r}_2, \mathbf{r}'_2) \times \\ \times \bar{\Psi}_{\text{inc}}(\mathbf{r}_1) \bar{\Psi}_{\text{inc}}^*(\mathbf{r}_2) d^3 r_1 d^3 r_2 d^3 r'_1 d^3 r'_2 \quad (59)$$

where $\bar{G}(\mathbf{r}'_1, \mathbf{R})$ is the mean propagator from \mathbf{r}'_1 (inside the medium) to \mathbf{R} (outside the medium), $\bar{\Psi}_{\text{inc}}(\mathbf{r}_1)$ is the normalized — mean incident field at \mathbf{r}_1 (inside the medium) and $\tilde{U}(\mathbf{r}_1, \mathbf{r}'_1, \mathbf{r}_2, \mathbf{r}'_2)$ is the sum of all scattering diagrams with ends stripped. Because the scatterers are in half space, \tilde{U} differs from U obtained in the bulk. However, we still have the relation between crossed and ladder diagrams, namely

$$\tilde{U}_R(\mathbf{r}_1, \mathbf{r}'_1, \mathbf{r}_2, \mathbf{r}'_2) = \tilde{F}(\mathbf{r}_1, \mathbf{r}'_1) \delta(\mathbf{r}_1 - \mathbf{r}_2) \delta(\mathbf{r}'_1 - \mathbf{r}'_2) \quad (60)$$

$$\tilde{U}_i(\mathbf{r}_1, \mathbf{r}'_1, \mathbf{r}_2; \mathbf{r}'_2) = \tilde{F}(\mathbf{r}_1, \mathbf{r}'_1) \delta(\mathbf{r}_1 - \mathbf{r}'_2) \delta(\mathbf{r}'_1 - \mathbf{r}_2) \quad (61)$$

which by Fourier transform gives a relation identical to that found for g_2 in the bulk (Eq. (56)). Using

$$\bar{\Psi}_{\text{inc}}(\mathbf{r}'_1) = e^{-z_1/\mu_0 \ell} e^{-i k s_i r_1} \\ \bar{G}(\mathbf{r}'_1, \mathbf{R}) = e^{-z_1/\mu \ell} \frac{e^{i k |\mathbf{R} - \mathbf{r}'_1|}}{4 \pi |\mathbf{R} - \mathbf{r}'_1|} \\ \approx e^{-z_1/\mu \ell} e^{-i k s_c r'_1} \frac{e^{-i k R}}{4 \pi R} \quad (62)$$

(with the notation of Sect. 2).

We obtain

$$\alpha(s_i, s_c) = \frac{1}{(4 \pi)^2 S} \int d^3 r d^3 r'_1 \cdot \tilde{F}(\mathbf{r}_1, \mathbf{r}'_1) e^{-\frac{z_1}{\mu_0 \ell}} \times \\ \times e^{-\frac{z'_1}{\mu \ell}} + \cos [k(s_i + s_c)(\mathbf{r}_1 - \mathbf{r}'_1)] e^{-\frac{(z_1 + z'_1) \mu_0 \mu}{2 \ell}} \quad (63)$$

Thus, as g_2 in a bulk system, α can be expressed in terms of the reducible diagrams only (at least to the leading order in λ/ℓ). Although \tilde{F} differs from F in the bulk (given in Appendix A), both quantities obey the same integral equation [5]. Comparison of this equation with equation (9) shows that $\tilde{F}(\mathbf{r}, \mathbf{r}') = \frac{4 \pi c}{\ell^2} P(\mathbf{r}, \mathbf{r}')$, where P has been defined in section 2. Thus, the final expression for the stationary albedo is identical to that derived in our phenomenological approach. Furthermore the present derivation will also allow us to study the coherent albedo as a function of the order of scattering without needing the introduction of time t as was necessary in section 2.

5. Expansion of the albedo as a function of the order of scattering.

The Fourier transform of the vertex function U_i has a diffusion pole which is the result of the summation of a geometric series whose generic term of order n represents the average value over all the scattering sequences of order $(n+2)$. It is therefore possible to study the contribution to the coherent backscattering cone associated with the order n of scattering. Let us start from the expression (63) of the albedo with the approximation $z = z' = \ell$ justified by the presence of the exponential terms. We rewrite the coherent contribution $\alpha_c(\theta)$ in the stationary regime ($\Omega = 0$):

$$\alpha_c(\theta) = \frac{3 \mu \mu_0 \ell}{(2 \pi)^3} \int d^2 \rho e^{-i \mathbf{k}_\perp \cdot \rho} \int d^3 q \frac{1}{\ell^2 q^2} \times \\ \times e^{i \mathbf{q}_\perp \cdot \rho} (1 - e^{2 i q_z (\ell + z_0)}). \quad (64)$$

The denominator $\ell^2 q^2$ is the sum $\sum_{n=0}^{\infty} (1 - (q\ell)^2)^n$ within the convergence radius $q\ell < 1$. Then:

$$\alpha_c(\theta) = \frac{3 \mu \mu_0 \ell}{(2 \pi)^3} \int d^2 \rho e^{-i \mathbf{k}_\perp \cdot \rho} \int_{q < 1/\ell} d^3 q \times \\ \times \sum_{n=0}^{\infty} (1 - (q\ell)^2)^n e^{-i \mathbf{q}_\perp \cdot \rho} (1 - e^{2 i q_z (\ell + z_0)}). \quad (65)$$

It must be noted that the cut-off $q\ell < 1$ associated with the convergence of the series cancels all the contributions to $\alpha_c(\theta)$ for which $k_\perp < 1/\ell$, i.e. for the angles $\theta > \lambda/2 \pi \ell$. Since the series converge uniformly, we can write:

$$\alpha_c(\theta) = \frac{3 \mu \mu_0 \ell}{2 \pi} \sum_{n=0}^{\infty} \int' d q_z \times \\ \times (1 - e^{2 i q_z (\ell + z_0)}) (1 - (k_\perp \ell)^2 - (q_z \ell)^2)^n \quad (66)$$

where the \int' represents a restriction to the

q_z values such that $q_z^2 < 1/\ell^2 - k_\perp^2$. Finally,

$$\alpha_c(\theta) = \frac{3 \mu \mu_0}{2 \pi} \sum_{n=0}^{\infty} I_n(\theta) \quad (67)$$

where

$$I_n(\theta) = \frac{2^{n+1} n!}{(2n+1)!!} (1 - (k_\perp \ell)^2)^{n+1/2} \times \left[1 - \frac{j_n \left[\frac{a}{\ell} \sqrt{1 - (k_\perp \ell)^2} \right]}{\left(\frac{a}{\ell} \sqrt{1 - (k_\perp \ell)^2} \right)^n} \right] \quad (68)$$

where $a = 2(\ell + z_0)$ and $j_n(x)$ is the spherical Bessel function of first kind. In equation (68), the coherent albedo appears as a superposition of the contributions $I_n(\theta)$, which represent the average over the diffusion paths with $(n+2)$ scatterings. Figure (7) shows how the lineshape of $\alpha_c(\theta)$ is obtained from the sum of all the I_n 's. It is also possible to obtain the lineshape of $I_n(\theta)$ for each value of n . It can be shown from the asymptotic expansion of the function j_n that the characteristic angle $\theta_n \simeq \lambda/2\pi\ell\sqrt{n}$ (for large n) measures the angular width in which the coherent contribution for the diffusion paths of order n is maximal. We therefore expect the paths of greater extent to contribute mainly to the small angle values of $\alpha_c(\theta)$. It would be therefore possible, within the limit of a perfect instrumental profile, to know the greatest coherent path by measuring directly the height of $\alpha_c(\theta)$.

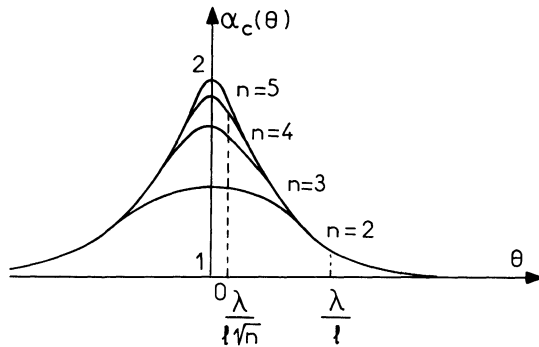


Fig. 7. — Contribution of the different orders of scattering to the coherent backscattering cone.

6. The polarization effects.

Until now, we have considered the case of scalar waves. The experimental results [10, 11] however indicate that the polarization effects associated with the vectorial nature of the electromagnetic field are important. Polarization modifies the albedo in two ways :

- i) it affects the time reversal invariance and therefore the interference effect ;
- ii) it modifies the relative weight of diffusion

paths both for the incoherent and coherent contributions.

Different approaches [8, 13] can be chosen in order to treat polarization effects. One of them consists in studying the solutions of Dyson and Bethe-Salpeter equations in a multiple scattering expansion for the amplitude of the wave and for its intensity. In this method the polarization effects are introduced by the relation.

$$E_i(\mathbf{r}) = \int_v d^3r' G_0(\mathbf{r} - \mathbf{r}') (\delta_{ij} - \hat{k}_i \hat{k}_j) E_j(\mathbf{r}') \quad (69)$$

where E_i and E_j are components of the electric field ($i, j = x, y, z$), $G_0(\mathbf{r} - \mathbf{r}')$ is the scalar Green function and \hat{k} is a unit vector along the emergent direction after the collision i.e. along $\mathbf{r} - \mathbf{r}'$. A multiple scattering expansion based on equation (69) leads to the study of a complicated tensor for which results can be obtained only within the diffusion approximation.

The main drawback, in our opinion, of this approach which was followed by Stephen and Cwlich [13] is that it is restricted to the case of pure Rayleigh scattering, i.e. to point-like scatterers. We shall use here a different approach which develops our former results [12, 23]. Although less rigorous, it allows the two different effects of polarization (i) and (ii) to be separated and can, therefore, be extended to finite size scatterers.

Let us first study the dominant effect (i), which is how the polarization affects the coherence. In a first step, we consider the case of pure Rayleigh scattering, for which the polarization vector \mathbf{P}' after a simple scattering event is :

$$\mathbf{P}' = \mathbf{k}' \times (\mathbf{k}' \times \mathbf{P}) \quad (70)$$

where \mathbf{k}' is the scattered wavevector and \mathbf{P} the incident polarization. This expression (70) leads directly to (69). Equation (70) is conveniently written in a matricial form, $\mathbf{P}' = \underline{M}(k') \mathbf{P}$, where \underline{M} is the 3×3 symmetric matrix :

$$\underline{M} = \begin{pmatrix} 1 - k_x^2 & -k_x k_y & -k_x k_z \\ -k_x k_y & 1 - k_y^2 & -k_y k_z \\ -k_x k_z & -k_y k_z & 1 - k_z^2 \end{pmatrix}. \quad (71)$$

Consider now the polarization state after a standard multiple scattering sequence of the type $\mathbf{k}_0 \rightarrow \mathbf{k}_1 \rightarrow \dots \rightarrow \mathbf{k}_n = -\mathbf{k}_0$, i.e. right in the backscattering direction. According to equation (71), the final polarization $\mathbf{P}_n^{(+)}$ after the sequence is :

$$\mathbf{P}_n^{(+)} \equiv \underline{A}^{(n)} \mathbf{P}_0 = \underline{M}_n \underline{M}_{n-1} \dots \underline{M}_1 \mathbf{P}_0 = \prod_{i=0}^n \underline{M}_{n-i} \mathbf{P}_0 \quad (72)$$

where we used $\underline{M}_0 \mathbf{P}_0 = \mathbf{P}_0$ and where $\underline{A}^{(n)}$ is the matrix relating $\mathbf{P}_n^{(+)}$ and \mathbf{P}_0 .

The polarization state $\mathbf{P}_n^{(-)}$ of the time-reversed sequence is given by the matrix $\prod_{i=0}^n \underline{M}_i$. For pure Rayleigh scattering the \underline{M} 's are symmetrical so that :

$$\mathbf{P}_n^{(-)} = \underline{A}^{(n)+} \mathbf{P}_0 \quad (73)$$

where $\underline{A}^{(n)+}$ is the transpose of $\underline{A}^{(n)}$.

We assume that \mathbf{P}_0 is along the z -axis and the incident wavevector \mathbf{k}_0 is along the x -axis, then we have :

$$\begin{cases} P_{nz}^{(+)} = P_{nz}^{(-)} = A_{zz}^{(n)} \\ P_{ny}^{(+)} = A_{yz}^{(n)} \\ P_{ny}^{(-)} = A_{zy}^{(n)}. \end{cases} \quad (74)$$

Therefore, for the parallel configuration where the emergent light is analysed along \mathbf{P}_0 , we have $P_{nz}^{(+)} = P_{nz}^{(-)}$ and the coherence in the backscattering direction is fully maintained for any n -step loop. As in the scalar case, the prefactor between the vector \mathbf{P} and the real field remains invariant by time reversal. It means that the expected enhancement between coherent and incoherent contribution is exactly two as for the scalar case.

This property remains valid for Rayleigh-Gans scattering by scatterers of arbitrary shape, or for Rayleigh scattering by particles of anisotropic polarisability. Indeed, in the first case, we have $\mathbf{P}' = M(\mathbf{k}') S(\mathbf{k}' - \mathbf{k}) \mathbf{P}$ where the scalar form factor $S(\mathbf{k}' - \mathbf{k})$ is time reversal invariant. In the second one, $\mathbf{P}' = M(k') \alpha(i) \mathbf{P}$ where $\alpha(i)$ is the symmetrical polarisability tensor of the (i -th) scatterer and the above demonstration can be straightforwardly extended.

In the more general case of Mie scattering, this simple demonstration cannot be applied as such because \mathbf{P}' depends on $\hat{\mathbf{k}}, \hat{\mathbf{k}}'$ and \mathbf{P} . However, at least for spherical scatterers, the above property remains valid, i.e. $P_n^{(-)} = \underline{A}^{(n)+} P_0$.

To show this, we note that, for a given scattering event, the components of polarization parallel and perpendicular to the scattering plane are multiplied by factors which depend both on $\hat{\mathbf{k}}$ and $\hat{\mathbf{k}}'$ only through $\cos(\hat{\mathbf{k}}, \hat{\mathbf{k}}')$. These factors are thus unaffected by reversing the way of propagation. Hence, we have :

$$P_n^{(+)} \equiv \underline{A}^{(n)} P_0 = \prod_{i=n}^1 R_{i+1}^{-1} N_i R_i^{-1} P_0 \quad (75)$$

where N_i is a diagonal matrix for the i -th Mie scattering event ($\mathbf{k}_{i-1} \rightarrow \mathbf{k}_i$) and R_{i+1} the matrix representing the rotation around $\hat{\mathbf{k}}_i$ mapping the $(\mathbf{k}_{i-1}, \mathbf{k}_i)$ plane onto the $(\mathbf{k}_i, \mathbf{k}_{i+1})$ plane (with R_1 (resp. R_{n+1}^{-1}) the rotation mapping the (yz) plane onto the $(\mathbf{k}_1, \mathbf{k}_0)$ plane (resp. $(\mathbf{k}_{n-1}, \mathbf{k}_0)$ plane) and similarly :

$$\mathbf{P}_n^{(-)} = \left(\prod_{i=1}^n R_i N_i R_{i+1} \right) \mathbf{P}_0 = \underline{A}^{(n)+} P_0 \quad (76)$$

so that the full coherence is preserved in the parallel configuration.

Finally we note that, for all cases discussed here, we used a far field expression for the scattered fields. This requires the distance between scatterers to be much larger than the wavelength. In the opposite case, the above arguments cannot be used except for pure Rayleigh scattering. In this situation the outgoing polarization P_1 after a single scattering event remains given at any distance, by a linear symmetric operator acting on the incoming polarization P_0 , which is the basis of coherence in the parallel configuration.

This full coherence does not generally occur in the case of perpendicular polarizers where the emergent light is analysed along the y -direction since in general the matrix $\underline{A}^{(n)}$ is not symmetric. An exception is when the scattering sequence is in a plane. In this case, which includes the double scattering situation in the backscattering direction, the matrix $\underline{A}^{(n)}$ is symmetric so that there is full coherence between a sequence and its time reverse counterpart. Apart from this particular case, there is no obvious relation between $\underline{A}_{ij}^{(n)}$ and $\underline{A}_{ji}^{(n)}$ so that the problem of perpendicular polarizers is complicated. However, for pure Rayleigh scattering, quantitative results can be obtained in the limit of large scattering sequences as we shall show now.

For perpendicular polarization we define the average coherence ratio : $C(n) \equiv \frac{\langle P_{n\perp}^{(+)} P_{n\perp}^{(-)} \rangle}{\langle P_{n\perp}^2 \rangle}$ between a pair of time reversed sequences in the perpendicular configuration over all the n -th ($n \geq 2$) order sequences. $P_n^{(+)}$ and $P_n^{(-)}$ are calculated by the two recursion relations obtained from equations (72) and (73) :

$$\begin{cases} P_{n\perp}^{(+)} = -k_{nx} k_{ny} A_{xz}^{(n-1)} + (1 - k_{ny}^2) P_{n-1,\perp}^{(+)} - k_{ny} k_{nz} P_{n-1,\perp}^{(+)} \\ P_{n\perp}^{(-)} = -k_{nx} k_{nz} A_{xy}^{(n-1)} - k_{ny} k_{nz} A_{yy}^{(n-1)} + (1 - k_{nz}^2) P_{n-1,\perp}^{(-)}. \end{cases} \quad (77)$$

For Rayleigh scattering in a bulk medium, the successive wavevectors are independent random variables, so that the averages over k_n and $A_{ij}^{(n)}$ can be separated. In our situation of a semi-infinite medium, with point-like scatterers, this separation of averages should remain valid for long enough paths. In this case, the constraints due to the interface (no crossing condition, last scatterer within a mean free path from the

interface) are expected of little importance and $C(n)$ calculated in the bulk can be extended to the semi-infinite medium. Under these assumptions, we have :

$$\langle P_{n\perp}^{(+)} P_{n\perp}^{(-)} \rangle = \frac{6}{15} \langle P_{n-1,\perp}^{(+)} P_{n-1,\perp}^{(-)} \rangle + \frac{1}{15} \langle A_{yy}^{(n-1)} A_{zz}^{(n-1)} \rangle . \quad (78)$$

Similarly, from equations (72) and (73)

$$\langle A_{yy}^{(n)} A_{zz}^{(n)} \rangle = \frac{1}{15} \langle P_{n-1,\perp}^{(+)} P_{n-1,\perp}^{(-)} \rangle + \frac{6}{15} \langle A_{yy}^{(n-1)} A_{zz}^{(n-1)} \rangle \quad (79)$$

with initial conditions for $n = 1$ (single scattering), $A_{yz}^{(1)} = 0$ and $A_{zz}^{(1)} = A_{yy}^{(1)} = 0$, the solution of this linear system gives :

$$\langle P_{n\perp}^{(+)} P_{n\perp}^{(-)} \rangle = \frac{1}{2} \left[\left(\frac{7}{15} \right)^{n-1} - \left(\frac{5}{15} \right)^{n-1} \right] . \quad (80)$$

To calculate the correlation ratio $C(n)$, we need an expression for $\langle P_{n\perp}^2 \rangle$ which is given by the solution of the recursion relations :

$$\begin{cases} \langle P_{n\parallel}^2 \rangle = \langle k_{nx}^2 k_{nz}^2 \rangle \langle (A_{xz}^{(n-1)})^2 \rangle + \langle k_{ny}^2 k_{nz}^2 \rangle \langle P_{n-1,\perp}^2 \rangle + \langle (k_{nz}^2 - 1)^2 \rangle \langle P_{n-1,\parallel}^2 \rangle \\ \langle P_{n\perp}^2 \rangle = \langle k_{nx}^2 k_{ny}^2 \rangle \langle (A_{xz}^{(n-1)})^2 \rangle + \langle (1 - k_{ny}^2)^2 \rangle \langle P_{n-1,\perp}^2 \rangle + \langle k_{ny}^2 k_{nz}^2 \rangle \langle P_{n-1,\parallel}^2 \rangle \\ \langle (A_{xz}^{(n)})^2 \rangle = \langle (1 - k_{nx}^2)^2 \rangle \langle (A_{xz}^{(n-1)})^2 \rangle + \langle k_{nx}^2 k_{ny}^2 \rangle \langle P_{n-1,\perp}^2 \rangle + \langle k_{nx}^2 k_{nz}^2 \rangle \langle P_{n-1,\parallel}^2 \rangle . \end{cases}$$

Solution of this linear system with initial conditions $P_{1\parallel}^2 = 1$, $P_{1\perp}^2 = 0$ and $A_{xz}^{(1)} = 0$ is :

$$\begin{cases} \langle P_{n\parallel}^2 \rangle = \frac{1}{3} \left(\frac{10}{15} \right)^{n-1} + \frac{2}{3} \left(\frac{7}{15} \right)^{n-1} \\ \langle P_{n\perp}^2 \rangle = \frac{1}{3} \left(\frac{10}{15} \right)^{n-1} - \frac{1}{3} \left(\frac{7}{15} \right)^{n-1} . \end{cases} \quad (82)$$

Equations (80) and (82) give :

$$C(n) = \frac{3}{2} \cdot \frac{(0.7)^{n-1} - (0.5)^{n-1}}{1 - (0.7)^{n-1}} . \quad (83)$$

Also equation (82) gives the depolarization ratios, which measure the transfer of intensity from the incident light polarized along \mathbf{P}_0 to the perpendicular component. They are defined by :

$$\begin{cases} d_{n\parallel} \equiv \frac{\langle P_{n\parallel}^2 \rangle}{\langle P_{n\parallel}^2 \rangle + \langle P_{n\perp}^2 \rangle} = \frac{1 + 2(0.7)^{n-1}}{2 + (0.7)^{n-1}} \\ d_{n\perp} \equiv \frac{\langle P_{n\perp}^2 \rangle}{\langle P_{n\perp}^2 \rangle + \langle P_{n\parallel}^2 \rangle} = \frac{1 - (0.7)^{n-1}}{2 + (0.7)^{n-1}} . \end{cases} \quad (84)$$

As expected they converge to the same limit 1/2 for n going to infinity.

The correlation ratio $C(n)$ varies from 1 for $n = 2$ where $P_{2\perp}^{(+)} = P_{2\perp}^{(-)}$ to zero for n going to infinity, where $C(n) \sim (0.7)^n$. This exponential damping has an effect on the lineshape analogous to that of the absorption effect. But the quantitative result (Eq. (83)) is by no mean universal. It has only been derived for point-like scatterers for which the successive scatterings are statistically independent.

The knowledge of $C(n)$ tells us that the enhancement in the backscattering direction is less than two.

In order to predict its value we also need to know how the polarization affects the weight of light paths [point (ii)]. Equations (84) show that $d_{n\perp}$ increases only slowly to 1/2 (for $n = 10$, for instance it is still 0.47). It indicates that the transfer of intensity from the incident polarization towards the crossed one is a rather slow process which must be therefore taken into account. $I(n, \theta)$ representing the contribution of paths of length $L = n\ell^*$ to the total incoherent intensity (for both polarization directions), we thus write for the ratio of the coherent to the incoherent albedo in the perpendicular polarization state :

$$\frac{\alpha_c^\perp(\theta)}{\alpha_{inc}^\perp} = \frac{\sum_{n \geq 1} d_{n\perp} C(n) I(n, \theta)}{\sum_{n \geq 1} d_{n\perp} I(n, \theta)} \quad (85)$$

where we made the approximation that $d_{n\perp}$ is unaffected by the interface (which is right for large enough value of n). A further assumption is to use for $I(n, \theta)$ the result of the scalar diffusion approximation (Eq. (15)). In this case, for the smallest scatterers studied experimentally (diameter $d = 0.11 \mu\text{m}$) the above expression gives $\frac{\alpha_c^\perp(\theta = 0)}{\alpha_{inc}^\perp} \approx 0.14$ in good agreement with the experiments.

The above expressions allow us to discuss the lineshape of the coherent backscattering peaks. We have :

$$\alpha_c^\parallel(\theta) \propto \sum_n d_{n\parallel} I(n) e^{-\frac{n}{3} \left(\frac{2\pi\ell}{\lambda} \right)^2 \theta^2} \quad (86)$$

$$\alpha_c^\perp(\theta) \propto \sum_n (1 - d_{n\parallel}) I(n) C(n) e^{-\frac{n}{3} \left(\frac{2\pi\ell}{\lambda}\right)^2 \theta^2}. \quad (87)$$

Where we separated in $I(n, \theta)$ the incoherent contribution $I(n) \propto n^{-3/2}$ and the angular dependent part $\exp\left(-\frac{n}{3} \left(\frac{2\pi\ell}{\lambda}\right)^2 \theta^2\right)$ obtained for scalar waves within the diffusion approximation. These relations for the coherent albedo in the parallel and in the perpendicular configurations can be compared with those obtained by Stephen and Cwillich [13]. To do that, let us write :

$$d_{n\parallel} = \frac{1}{2} + \frac{3}{2} \frac{(0.7)^n}{2 + (0.7)^n} \approx \frac{1}{2} + \frac{3}{4} (0.7)^n$$

and

$$C(n) \approx \frac{3}{2} (0.7)^n.$$

Then α_c^\parallel appears as the sum of two contributions :

$$\alpha_c^\parallel(\theta) = \alpha_c^{\text{(scal)}}(\theta) + \frac{3}{4} \sum_n I(n) \times e^{-n \ln(0.7) - \frac{n}{3} \left(\frac{2\pi\ell}{\lambda}\right)^2 \theta^2} \quad (88)$$

where $\alpha_c^{\text{(scal)}}(\theta)$ is the contribution already found for scalar waves (cf. Eq. (18)) while the second broader contribution comes from the fact that for short paths, the intensity contained in the parallel component is larger than that corresponding to full depolarization.

In a similar way, we find that α_c^\perp is the difference of a « scalar » broad contribution and another positive contribution again due to the transfer of intensity from the parallel to the perpendicular component.

Although it is less systematic, our approach is interesting because it shows the origin of the second component found by Stephen and Cwillich [13]. It is due to the transfer of intensity between different polarizations. For the case of large scatterers where this transfer is completed over a distance of the order of the *transport* mean free path [10], it should be absent.

Let us stress again that our approach gives only qualitative results in the sense that for short paths the expressions of $d_{n\parallel}$, $C(n)$ and $I(n, \theta)$ are not accurate. But for the same reasons the treatment based on a multiple scattering expansion within the diffusion approximation cannot give better results. Furthermore, unlike what is implicitly assumed in equations (85) and (87), the weight of short paths is an anisotropic function of the distance \mathbf{r} between the first and last scatterers. This is obvious for double scattering where the emergent polarization is zero when \mathbf{r} is parallel to the incident polarization but not for other directions \mathbf{r} . This anisotropy implies an

anisotropy of the parallel backscattering cone as was demonstrated experimentally and analysed by Van Albada *et al.* [14].

Therefore, any discussion of the lineshape at large angles should start from an exact calculation of the low order contributions of the Rayleigh scattering rather than from a treatment within the diffusion approximation. This should be contrasted with the behaviour at small angles. For scatterers of any size, $d_{n\parallel}$ tends to 1/2 for large n , so that the parallel lineshape has exactly the same triangular singularity as in the scalar case, while the perpendicular lineshape is rounded by the term $C(n)$, in a way similar to the one caused by absorption.

7. Albedo of a fractal system.

Let us consider a fractal system such that the light propagates in a fractal structure. For instance, one could imagine, a percolation system built up by metallic and transparent balls of relative concentration p , randomly mixed in a container. Let us assume that the light is not absorbed within the transparent clusters while it cannot propagate through the metallic particles. Moreover, the concentration p is adjusted to the threshold value p_c in order to spread out the fractal structure over the whole sample. At p_c , the percolating cluster and finite size clusters coexist. The light is therefore scattered by these two types of clusters which both contribute to the lineshape of the albedo. Nevertheless, the multiple scattering within the finite size clusters is of low order (small diffusion paths) and therefore contributes to the large angle values of the albedo. On the opposite the multiple scattering inside the percolating cluster will probe the fractal structure at any order and represents the main contribution to the lineshape of the coherent albedo. It is this situation that we analyse now.

It is known that the diffusion on a fractal structure is anomalous and can be characterized by the spectral dimension \tilde{d} in addition to the fractal (or Hausdorff) dimension \bar{d} of the structure. More precisely, the probability for a particle to diffuse over a distance r from the source at time t is believed to obey a homogeneous function due to scaling invariance

$$P(r, t) \propto \frac{1}{\Lambda_t^{\tilde{d}}} f\left(\frac{r^2}{\Lambda_t^2}\right) \quad (89)$$

where Λ_t is the anomalous diffusion length for time t :

$$\Lambda_t \propto t^\nu \text{ and } \nu = \frac{\tilde{d}}{2\bar{d}} \left(\nu < \frac{1}{2}\right). \quad (90)$$

How is it possible to handle the escape of light through the interface ? First there is a purely geometric aspect : the fractal structure of the interface of a

given fractal can be quite different from the bulk structure. A regular fractal object such as the Sierpinski systems can be cut by a plane in different ways. The distribution of the transparent particles can be characterized generally by a fractal dimension of the surface $\bar{d}_s \leq \bar{d}$. In addition to this new fractal dimension \bar{d}_s , the coherence length ξ of the fractal structure can be strongly reduced within the plane cut, as in the case of percolation where only finite clusters exist at the threshold p_c of three-dimensional sample. Finally, an important and delicate problem occurs when the effect of the escape through the interface is taken into account. The image trajectories must be supported by the image structure mirrored by the interface plane. For the case of a symmetry plane in regular fractals (the bisector plane of the Sierpinski tetrahedron network for instance) the image structure coincides with the network and the probability law given by equation (89) can be applied for both the terminal point of the random walk and its image. For random fractals like the infinite percolative cluster, this property is only true on average. By neglecting the possible departure from this average property, we will use subsequently the image method for the transfer probability from ρ at time t :

$$\tilde{P}(\rho, t) \propto \frac{1}{\Lambda_t^{\bar{d}}} \left[f\left(\frac{\rho^2}{\Lambda_t^2}\right) - f\left(\frac{\rho^2 + \ell^{*2}}{\Lambda_t^2}\right) \right] \quad (91)$$

and for large t :

$$\tilde{P}(\rho, t) \propto \frac{1}{\Lambda_t^{\bar{d}+2}} g\left(\frac{\rho^2}{\Lambda_t^2}\right).$$

It is now straightforward to calculate the stationary transfer function [23]

$$\tilde{Q}(\rho) \equiv \int_{\tau}^{\infty} dt \tilde{P}(\rho, t) \propto \frac{1}{\rho^{\eta}} \quad (92)$$

where $\eta = \bar{d} + 2 - \frac{1}{\nu}$.

The convergence of the integral in (92) is ensured when $\eta > 0$ and since $\nu < 1/2$ one finds that $\eta < \bar{d}$. The final step consists in calculating the simplified expression of the albedo $\alpha(q)$ by the Fourier transform in the fractal subspace of dimension \bar{d}_s of the stationary transfer function $Q(\rho)$:

$$\alpha(q) \propto \int d^{\bar{d}_s} \rho e^{iq_{\perp} \cdot \rho} \tilde{Q}(\rho). \quad (93)$$

As far as $\zeta \equiv \eta - \bar{d}_s > 0$, $\alpha(q)$ is finite and proportional to

$$\alpha(q) \propto (1 - (q\ell^*)^{\zeta}). \quad (94)$$

For Euclidean space one finds again the triangular

shape of the peak since $d = \bar{d}$, $\bar{d}_s = \bar{d} - 1$, $\nu = 1/2$ and $\zeta = 1$. Since η is bounded by \bar{d}_s and \bar{d} , one finds that $0 < \zeta < \bar{d} - \bar{d}_s$, the last bound $\bar{d} - \bar{d}_s = 1$ for Euclidian space. The limiting case of $\zeta = 0$ leads to an unphysical logarithmic divergence of the albedo. Its origin lies in the fact that the stationary regime cannot be defined as in the case of the two-dimensional diffusion constant in the Anderson localization problem. A more detailed analysis of this regime will be published elsewhere. In the general case ($\zeta \neq 0$) the shape of the backscattering peak of a fractal analysed by the previous expressions is sharper than the linear peak (cf. Fig. 8). Its measure would produce a determination of ζ and therefore \bar{d} if \bar{d} and \bar{d}_s are known otherwise. This short analysis emphasizes the interest of the albedo experiment to characterize heterogeneous materials with a possible fractal structure.

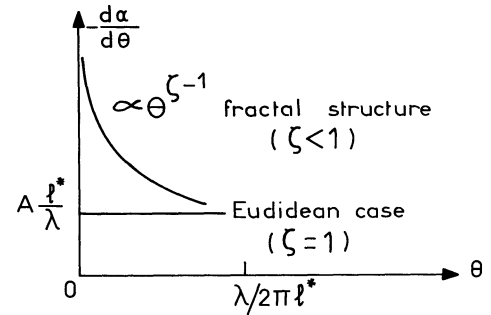


Fig. 8. — Comparison of the slope of the coherent backscattering cone for a fractal structure and a Euclidian space. For the latter case $A = 25/6$ (cf. Eq. (35)).

8. Conclusion.

Let us summarize the main results of this article. We have developed a detailed analysis of the coherent backscattering contribution to the reflection coefficient of a semi-infinite disordered medium (albedo). Within the framework of the weak localization approximation, valid for weakly scattering systems, we have established an analytical expression of the albedo for various situations including time-dependent effects, absorption, intensity modulation, anisotropic scattering, polarization and propagation in fractal structures.

In section 2, we have discussed a heuristic expression for the time-dependent albedo. Its stationary limit corresponds to the expression established by Tsang and Ishimaru [5]. We have analysed in detail the different characteristic time-scales of the problem: the elastic mean free time τ , the time τ_B for the Brownian motion of the scatterers over a wavelength and the relaxation time of the phase $\sqrt{\tau \tau_B}$.

We have explained the rounding effects observed on the coherent albedo in presence of absorption or for the case of amplitude modulation of the incident wave.

We have then presented a generalization of the albedo to the more realistic case of anisotropic scatterers. It is based on a treatment of the classical transport equation within the diffusion approximation. The previous expression is unchanged except for the replacement of the elastic mean free path ℓ by the transport mean free path ℓ^* .

A microscopic derivation of the coherent albedo is given in sections 3 and 4. It is based on the Bethe-Salpeter equation for the intensity. It represents another way to justify the heuristic expression as well as a demonstration of the existence of the interference factor $\cos(\mathbf{k}_i + \mathbf{k}_c) \cdot (\mathbf{r}_1 - \mathbf{r}_N)$ between time-reversed paths. It is actually established rigorously for scalar waves and point-like scatterers to first order in λ/ℓ . The series expansion of the coherent albedo in terms of the order of scattering has also been obtained, which shows directly how the Gaussian contributions add together to build up the triangular singularity in the backscattering direction.

Polarization effects associated with the vectorial nature of the light are treated in detail in section 6. Two main effects have been considered: how the polarization affects the coherent effect, and how it modifies the weight of diffusion paths for both coherent and incoherent contributions. A general method is presented but calculations are performed for the case of Rayleigh scattering only. We recover previous results. Moreover, our method which decouples the polarization effects and transport phenomena allows us to discuss the case of finite size scatterers.

Finally the problem of the albedo of a fractal structure has been considered in section 7. A new expression has been obtained for the coherent albedo using the simplified boundary condition given by the image method. Near the backscattering direction, the lineshape varies with the angle θ as a power law involving a new exponent related to the fractal dimensions (surface and volume) and the spectral dimension.

The present work as well as other recent theoretical and experimental studies suggest that the coherent backscattering phenomenon of light is well understood. Nevertheless, some points remain unclear. First, experiments show an enhancement factor in the backscattering direction between 1.8 and 1.9 instead of 2 after various corrections are taken into account. Second, the behaviour at large angles corresponding to small paths is not correctly described by our heuristic formula. Let us try to classify the different situations according to their difficulty.

i) *Scalar waves and point-like scatterers*: This is the simplest situation. In this regime, the diffusion approximation is justified at small angles, but at large angles the diffusion paths involved are short so that it becomes invalid as well as the « image » boundary conditions.

ii) *Polarized light and point-like scatterers*: The approximate expression of the albedo works at small angles as previously but, in addition to i), the strong correlation between wavevectors after each scattering for small values of the scattering order and the correct boundary condition for vectorial waves at the interface are new reasons for the standard formula to be invalid at large angles ($q\ell > 1$).

iii) *Scalar waves and non point-like scatterers*: The generalization of the expression in section 2.d explains correctly the change of the slope of the albedo at small angles from ℓ to ℓ^* . But even with a boundary condition more realistic than the usual image method the behaviour at large angles is unphysical. However, it still relies on the diffusion approximation.

iv) *Polarized light and non point-like scatterers*: We described this regime by the replacement of ℓ by ℓ^* keeping the previous expressions unchanged. Surprisingly, despite the various approximations used (image method near the interface, neglect of the correlation between scattering angles, anisotropic scattering, etc.) our expressions are in good agreement with the experiments [10].

Some additional problems have not been taken into account. First, the factor 2, i.e. the height of the backscattering peak, is measured relatively to the large angle value. However, this asymptotic value may differ from the incoherent intensity since it includes the coherent contribution of multiple scattering sequences along closed loops which do not depend on the angle. Moreover, along the same direction, we do not know whether, in media with strong dielectric contrast, the scattering processes near the interface are not only due to the scatterers but also to the interface which at very small distances (smaller than ℓ) may behave like a mirror.

For dense media, additional problems like spatial correlations of the scatterers have not been taken into account. They have been recently considered in the simplest approximation [24]. The corrections to the averaged propagator \bar{G} to higher order in λ/ℓ are also important. Such corrections are due to repeated scattering of the wave on nearest neighbour scatterers which become relevant in dense media. The latter corrections can be at the origine of a maximum value smaller than 2. Beyond the weak localization regime one enters the critical regime of Anderson's localization. Important predictions have been formulated [25] for the scaling invariance of the

optical properties of the medium such as the transmission coefficient. Despite a recent attempt in this way [26], there is no experimental confirmation so far. In this critical regime all transport coefficients are affected by the strong localization phenomenon : they must be reformulated as scaling functions of length or time over renormalized diffusion length. The boundary condition at the interface must also be treated carefully. Both these remarks indicate that the coherent albedo is probably a relevant property in the critical regime. Special treatment will be necessary to derive the expression of the albedo for this regime, which will be reported elsewhere.

Appendix A.

EXPRESSION OF THE AVERAGED PROPAGATOR \bar{G} IN A DISORDERED MEDIUM. — In a disordered medium where the refractive index is a fluctuating variable the propagator $G(\omega, \mathbf{r}, \mathbf{r}_0)$ is solution of the equation

$$[\nabla_r^2 + k_0^2(1 + n(\mathbf{r}))] G(\omega, \mathbf{r}, \mathbf{r}_0) = \delta(\mathbf{r} - \mathbf{r}_0) \quad (\text{A.1})$$

which is the equation (36) given in the text. An iterative solution of equation (A.1) can be obtained by an expansion as a function of the potential $V(r) \equiv k_0^2 n(r)$. If $G(\omega, \mathbf{p})$ is the Fourier transform of $G(\omega, \mathbf{r}, \mathbf{r}_0)$, we have :

$$\begin{aligned} G(\omega, \mathbf{p}) &= \\ &= G_0(\omega, \mathbf{p}) + G_0(\omega, \mathbf{p}) V(\mathbf{q} = 0) G_0(\omega, \mathbf{p}) + \\ &\quad + G_0(\omega, \mathbf{p}) \sum_{\mathbf{q}} V(\mathbf{q}) G_0(\omega, \mathbf{p} + \mathbf{q}) \\ &\quad \times V(-\mathbf{q}) G_0(\omega, \mathbf{p}) + \dots \end{aligned} \quad (\text{A.2})$$

$$\begin{aligned} \bar{G}(\omega, \mathbf{p}) &= G_0(\omega, \mathbf{p}) + G_0(\omega, \mathbf{p}) NV(0) G_0(\omega, \mathbf{p}) + \\ &\quad + N \sum_{\mathbf{q}} G_0(\omega, \mathbf{p}) V(\mathbf{q}) G_0(\omega, \mathbf{p} + \mathbf{q}) V(-\mathbf{q}) G_0(\omega, \mathbf{p}) \\ &\quad + G_0(\omega, \mathbf{p}) NV(0) G_0(\omega, \mathbf{p}) NV(0) G_0(\omega, \mathbf{p}) + \dots \end{aligned} \quad (\text{A.3})$$

which is represented by the diagrammatic expansion of figure 10. It is now convenient to introduce the Dyson equation. Let us recall, it consists to classify the different diagrams appearing in figure 10 in reducible and irreducible diagrams. The sum of irreducible diagrams gives the averaged self-energy $\bar{\Sigma}(p, \omega)$. Equation (A.3) can be rewritten as :

$$\bar{G}(\omega, \mathbf{p}) = G_0(\omega, \mathbf{p}) + G_0(\omega, \mathbf{p}) \bar{\Sigma}(\omega, \mathbf{p}) \bar{G}(\omega, \mathbf{p}). \quad (\text{A.4})$$

The problem of calculating $\bar{G}(\omega, \mathbf{p})$ reduces to the calculation of $\bar{\Sigma}(\omega, \mathbf{p})$. A perturbation expansion of $\bar{\Sigma}(\omega, \mathbf{p})$ as a function of the impurity concentration n_i is given in figure 11. One of the main motivations

Equation (A.2) can be conveniently represented by the diagrammatic expansion of figure 9. The difference between this expansion and the usual one impurity expansion is that the potential is now a random variable due to the random position of

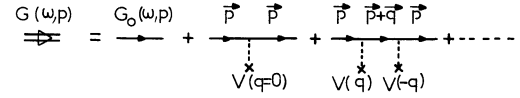


Fig. 9. — Diagrammatic expansion of the propagator G in a disordered medium.

scattering centres within the medium. Let us rewrite the potential $V(\mathbf{r})$ as

$$V(\mathbf{r}) = k_0^2 n(\mathbf{r}) = k_0^2 \sum_i n(\mathbf{r} - \mathbf{r}_i)$$

where $n(\mathbf{r} - \mathbf{r}_i)$ is the refractive index of one scattering centre. The Fourier transform becomes $V(\mathbf{q}) = k_0^2 n(\mathbf{q}) \rho_{\mathbf{q}}$ where the random variable $\rho_{\mathbf{q}}$ is defined by $\rho_{\mathbf{q}} = \sum_i e^{i\mathbf{q} \cdot \mathbf{x}_i}$. To obtain the averaged propagator $\bar{G}(\omega, \mathbf{p})$ we have to average equation (A.1). There appears expressions like :

$$\begin{aligned} \bar{\rho}_{\mathbf{q}} &= \frac{1}{\text{vol}} \prod_{i=1}^N \int d^3x_i \sum_j e^{i\mathbf{q} \cdot \mathbf{x}_j} = \frac{N}{\text{vol}} \int d^3x e^{i\mathbf{q} \cdot \mathbf{x}} \\ &= N \delta_{\mathbf{q}, 0} \overline{\rho_{\mathbf{q}} \rho_{-\mathbf{q}}} = N + N^2 \delta_{\mathbf{q}, 0} \end{aligned}$$

where N is the number of scattering centres. It gives for $\bar{G}(\omega, \mathbf{p})$ the expansion :

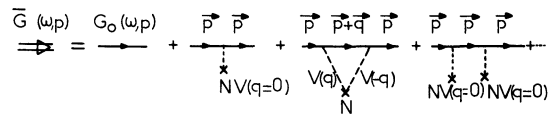


Fig. 10. — Diagrammatic expansion of the averaged propagator \bar{G} .

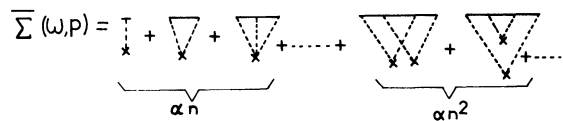


Fig. 11. — Diagrammatic expansion of the averaged self-energy $\bar{\Sigma}$ as a function of the impurity concentration n .

of this appendix is now to describe exactly the assumptions underlying the usual calculation of $\bar{\Sigma}(\omega, \mathbf{p})$ leading to the equation (41) given in the text.

We usually keep only the terms proportional to the impurity concentration eliminating the contributions of higher orders. A standard calculation gives after summation of the series :

$$\bar{\Sigma}(\omega, \mathbf{p}) = n_i T(\mathbf{p}, \mathbf{p}) \quad (\text{A.5})$$

where $T(\mathbf{p}, \mathbf{p})$ is the scattering T -matrix element associated with scattering on only one impurity. The optical theorem tells us that the cross-section σ is given by $\sigma = -\text{Im } T(\mathbf{p}, \mathbf{p})$ such that we obtain an averaged propagator \bar{G} attenuated on an elastic mean-free path given by $\frac{\ell}{2} = \frac{1}{2n_i\sigma}$. This approxi-

mation in $\bar{\Sigma}$ is therefore equivalent to consider scattering on only one effective impurity. It is important to note here what is the contribution of the diagrams we have neglected like those pictured in figure 11. The first one, proportional to n_i^2 is given by :

$$\begin{aligned} N^2 \sum_{\mathbf{q}_1, \mathbf{q}_2} V(\mathbf{q}_1) G_0(\omega, \mathbf{p} + \mathbf{q}_1) V(\mathbf{q}_2) \times \\ \times G_0(\omega, \mathbf{p} + \mathbf{q}_1 + \mathbf{q}_2) V(-\mathbf{q}_1) \\ \times G_0(\omega, \mathbf{p} + \mathbf{q}_2) V(-\mathbf{q}_2) \end{aligned}$$

and corresponds to repeated scattering between two impurities. This correlation restricts the angular integration over \mathbf{q}_2 to values such that $\cos \theta_2 \in \left[-\frac{\lambda}{4\pi\ell}, +\frac{\lambda}{4\pi\ell} \right]$ where ℓ is the elastic mean free path defined above. After some lengthy but straightforward calculations we find that the contribution of this diagram to the imaginary part of $\bar{\Sigma}$ is $AN^2|V|^4 \frac{\lambda}{\ell}$ where A is some numerical constant. The relative value between the first order and this contribution is given by $An_i|V|^2 \frac{\lambda}{\ell}$. It is therefore negligible for very dilute systems since the ratio λ/ℓ is very small. Nevertheless, we have to keep in mind that it exists if we want to calculate higher-order corrections to the diffusion constant or of other transport coefficients. It also becomes very important if one considers time-dependent scattering and resonances and how it affects the coherent backscattering phenomenon.

Appendix B.

SUMMATION OF THE MAXIMALLY CROSSED DIAGRAMS IN THE STATIONARY REGIME. — Since the pioneering work of Langer and Neal [27] on the singularity of the expansion of transport coefficients as a function of impurity concentration, many deriva-

tions have been given for the resummation of the maximally crossed diagrams for electronic systems (see e.g. Ref. [6]). For the case of the propagation of phonons in disordered systems, it has also been derived [28] in the hydrodynamic limit $q\ell(\omega) \ll 1$ and $\Omega\tau(\omega) \ll 1$ where q and Ω represent respectively the transfer of momentum and of energy between the two-interfering propagators.

In this appendix, we would like to give the sum of maximally crossed diagrams in a stationary regime but for any value of the momentum q , i.e. outside the diffusion approximation. As shown in reference [28] the sum of the geometric series associated with irreducible maximally crossed diagrams is given by :

$$U_i(\mathbf{k}, \mathbf{k}') = \frac{b^2 I(\omega, q)}{1 - bI(\omega, q)} \quad (\text{B.1})$$

where in the stationary regime $\Omega = 0$. Moreover, $b = \frac{n_i\sigma}{4\pi} = \frac{1}{4\pi\ell}$ and

$$I(\omega, q) \equiv \frac{2\pi^2}{V} \sum_{\mathbf{k}} \bar{G}(\omega, \mathbf{k}) \bar{G}^*(\omega, \mathbf{k} - \mathbf{q})$$

where $\mathbf{q} = \mathbf{k} + \mathbf{k}'$ is the transfer momentum. The Parseval theorem gives :

$$I(\omega, q) = \frac{1}{4\pi} \int d^3r e^{-i\mathbf{q}\cdot\mathbf{r}} \bar{G}(\omega, \mathbf{r}) \bar{G}^*(\omega, \mathbf{r}). \quad (\text{B.2})$$

The averaged propagator \bar{G} is given by equation (41) in the text :

$$\bar{G}(\omega, r) = \frac{1}{4\pi r} e^{ir\frac{\omega}{c} - r/\ell}$$

such that

$$I(\omega, q) = \frac{1}{4\pi} \int d^3r e^{-i\mathbf{q}\cdot\mathbf{r}} \cdot \frac{e^{-r/\ell}}{r^2}$$

or

$$I(\omega, q) = \frac{1}{q} \text{Arctg}(q\ell).$$

The sum of maximally crossed diagrams is then given by :

$$U_i(\omega, q) = \frac{1}{4\pi\ell} \cdot \frac{\text{Arctg } q\ell}{q\ell - \text{Arctg } q\ell}. \quad (\text{B.3})$$

In the hydrodynamic limit $q\ell \ll 1$ we then recover the usual result :

$$U_i(\omega, q) \underset{q \rightarrow 0}{\sim} \frac{3}{4\pi\ell} \cdot \frac{1}{\ell^2 q^2}$$

which corresponds to the diffusion approximation used in the text.

References

- [1] SCHUSTER, A., *Astrophys. J.* **21** (1905) 1.
- [2] DE WOLF, D. A., *IEEE Trans Antennas Propag.* **19** (1971) 254.
- [3] KUGA, Y., ISHIMARU, A., *J. Opt. Soc. Am.* **A 8** (1984) 831 and
KUGA, Y., TSANG, L., ISHIMARU, A., *J. Opt. Soc. Am.* **A 2** (1985) 616.
- [4] TSANG, L., ISHIMARU, A., *J. Opt. Soc. Am.* **A 1** 836 (1984).
- [5] TSANG, L., ISHIMARU, A., *J. Opt. Soc. Am.* **A 2** (1985) 1331.
- [6] ALTSHULER, B. L., ARONOV, A. G., KHMELNITSKII, D. E. and LARKIN, A. I., in *Quantum theory of Solids*, Ed Lifshitz I. M. (Mir. Moscow, 1982) pp. 130-237.
- [7] SHARVIN, D. Yu and SHARVIN, Yu. V., *Zh. Eksp. Teor. Fiz. Pis'ma Rod.* **34** (1981) 285 [*JETP Lett.* **34** (1981) 272].
- [8] GOLUBENTSEV, A. A., *Zh. Eksp. Teor. Fiz.* **86** (1984) 47 [*Sov. Phys. JETP* **59** (1984) 26].
- [9] AKKERMANS, E., MAYNARD, R., *J. Phys. France Lett.* **46** (1985) L-1045.
- [10] WOLF, P. E., MARET, G., *Phys. Rev. Lett.* **55** (1985) 2696.
WOLF, P. E., AKKERMANS, E., MAYNARD, R., MARET, G., *J. Phys. France* **49** (1988).
- [11] VAN, ALBADA, M. P., LAGENDIJK, A., *Phys. Rev. Lett.* **55** (1985) 2692.
- [12] AKKERMANS, E., WOLF, P. E., MAYNARD, R., *Phys. Rev. Lett.* **56** (1986) 1471.
- [13] STEPHEN, M. J., CWILICH, G., *Phys. Rev.* **B 34** (1986) 7564.
- [14] VAN ALBADA, M. P., VAN DER MARK, M. B., LAGENDIJK, A., *Phys. Rev. Lett.* **58** (1987) 361.
- [15] MARET, G., WOLF, P. E., *Z. Phys.* **B 65** (1987) 409.
- [16] ETEMAD, S., THOMPSON, R., ANDREJCO, H. J., *Phys. Rev. Lett.* **57** (1986) 575.
- [17] KAVEH, H., ROSENBLUH, M., EDREI, I., FREUND, I., *Phys. Rev. Lett.* **57** (1986) 2049.
- [18] ISHIMARU, A., *Wave propagation and scattering in random media*, Vol. 1 (Academic Press : New York) 1978.
- [19] SCHWARZSCHILD, *Göttingen Nachrichten*, p. 41 (1906) and *Sitzungs Berichte d. Preuss. Akad.*, Berlin (1914) p. 1183.
- [20] MORSE, P. M. and FESHBACH, H., *Methods of Theoretical Physics* (Mc Graw-Hill Book Company, Inc.) 1953.
- [21] LARKIN, A. I., KHMELNITSKII, D. E., *Sov. Phys. Usp.* **25** (1980) 185 and BERGMANN, G. : *Phys. Rev.* **B 28** (1983) 2914.
- [22] VAN DER MARK, M. B., VAN ALBADA, M. P., LAGENDIJK, A., to be published.
- [23] AKKERMANS, E., Thèse de Doctorat, Grenoble (June 1986) (unpublished).
- [24] TSANG, L., ISHIMARU, A., *J. Opt. Soc. Am.* **A 2** (1985) 2187.
- [25] ANDERSON, P. W., *Philos. Mag.* **B 52** (1985) 505.
- [26] GENACK, A. Z., *Phys. Rev. Lett.* **58** (1987) 2043.
- [27] LANGER, J. S., NEAL, T., *Phys. Rev. Lett.* **16** (1966) 984.
- [28] AKKERMANS, E., MAYNARD, R., *Phys. Rev.* **B 32** (1985) 7850.
- [29] WATSON, G. H., FLEURY, P. A., MCCALL, S. L., *Phys. Rev. Lett.* **58** (1987) 945.
-